UCLA
UCLA Electronic Theses and Dissertations

Title

3-Dimensional Morphologic Analysis of the Craniofacial Skeletal Complex Using Geometry-Based Superimposition and Normalization

Permalink

Author

Sung, Jay Hyuck

Publication Date

2013

Peer reviewed|Thesis/dissertation

UNIVERSITY OF CALIFORNIA

Los Angeles

3-Dimensional Morphologic Analysis of the Craniofacial Skeletal

Complex Using Geometry-Based Superimposition and

Normalization

A thesis submitted in partial satisfaction of the requirements

for the degree Master of Science in Oral Biology

by

Jay Hyuck Sung

2013

ABSTRACT OF THE THESIS

3-Dimensional Morphologic Analysis of the Craniofacial Skeletal Complex Using

Geometry-Based Superimposition and Normalization

by

Jay Hyuck Sung

Master of Science in Oral Biology

University of California, Los Angeles, 2013

Professor Sotirios Tetradis, Co-chair

Professor Won Moon, Co-chair

Introduction : Cephalometrics is a radiographic technique used to analyze craniofacial structures for diagnostic or analytic purposes. However, conventional cephalometrics has many limitations, including the fact that it is entirely landmark-dependent and based on a 2-dimensional image. In previous studies, Fourier descriptors have been used to describe part of the craniofacial structure. However, these studies are insufficient providing a complete set of information to fully

analyze craniofacial morphology. The aim of this study is to develop a true 3-dimensional description of the craniofacial structure that will provide the basis of morphologic analysis in a more comprehensive and effective way.

Materials and Methods : CBCT images taken at UCLA School of Dentistry by the Newtom 3G CBCT scanner (Image Works) were collected. Samples with significant craniofacial defects were excluded. Using 10 samples without morphologic abnormality, the curved outline of the craniofacial structure was defined by collecting the coordinates of the points along the border of the shape. The superimposition and averaging was done using procrustes analysis. Geometric algebraic methods were used to combine all the curved outlines to construct an average shape of the whole craniofacial structure allowing for superimposition and comparison.

Results : The outline of the skull was successfully aligned in 3-dimensional space to represent the craniofacial structure. The normalized form provided a basis for the comparison of an individual sample to the group average. The new method showed advantages over the conventional cephalometrics by eliminating the constraint factors of 2-dimensional images. This allows us to analyze difference and irregularities of craniofacial morphology in a more accurate and effective way.

Conclusion : The curve and surface information extracted from CBCT image data could be used to find a normalization of the population, which is a basis for a 3-dimensional cephalometric analysis to overcome the limitations of conventional cephalometry.

The thesis of Jay Sung is approved.

Ki-Hyuk Shin

Reuben Kim

Sotirios Tetradis, Committee Co-Chair

Won Moon, Committee Co-Chair

University of California, Los Angeles

2013

Table of Contents and Lists

1. Introduction

1-1.   Background of morphometric analysis

Evaluating the relationship of the structural components of the human face is an important diagnostic factor in Orthodontics, Maxillofacial, Craniofacial and Plastic surgery, Medical Anthropology and Dysmorphological genetics [1, 2]. In order to accomplish this task, radiographic techniques have been used for abstracting the human head into a measurable geometric scheme[3], allowing for comparison of morphology. This task of measuring the degree of similarity between forms, is based on the theories of Morphometrics. It has a long history[4] propelled by the desire to abstract form from the variety of organisms, dating from ancient Greece to a more modern study by D'Arcy Thompson[5] . In morphometric analysis, describing a shape is achieved by locating a finite number of points on each specimen which are called landmarks or pseudo-landmarks, and by evaluating their relationship to one another or to a pre-determined normative model.

In human craniofacial analysis, the traditional approach of morphometric analysis is known as Cephalometrics[6, 7]. It is based on a standardized radiographic image taken either from the Anterior-Posterior view or Lateral view. Conventional Cephalometric analysis involves two distinct features.

First, 'Multivariate Methods'[8] are mainly used to analyze the relationship between the landmarks, where distances or angles formed between landmarks are measured to represent shape. The form is often represented by a simplified triangular structure, and the covariance between a simple morphological trait and putative factors can be shown based on the measurements[9].

Although it is still commonly used in the biological literature [10-12], this indirect method of shape analysis can be less intuitive and even inaccurate because the shape representation by landmarks has been converted to combinations of ratios of lengths and angles. For this reason, It is argued that it is always easier to interpret pictures in the original space of the specimens than in some derived multivariate space[8].

Second, even when visual comparison is made in conventional cephalometrics, it is mainly based on 'edge superimposition[13]'. To study the difference in shapes and their averaging process require the step of registration and superimposition involving the elimination of arrangement factors[8]. Two shapes can rarely be superimposed perfectly, and different fitting criteria will generally yield different results[14]. 'Edge superimposition' is the most straightforward superimposition and involves matching a given edge between two landmarks of a planar figure to a common origin and direction(Fig. 1)[15]. In this method, the initial shape is reduced to the descriptor coordinates with respect to some convenient baseline. The most commonly used is the Na-Ba line, since it has been well known among the cephalometricians that the growth axis was perpendicular to the cranial base and that the cranial-base axis was the direction of least growth over this range[9].

However, such a baseline cannot be assumed to be consistent across different individuals, and therefore the majority of the studies in the literature are limited to the discussion of the superimposition of the same individual to show change over growth [16, 17] or a treatment process [18, 19]. In other cases, only a very basic level of visualization is possible(Fig. 2)[9, 20, 21].
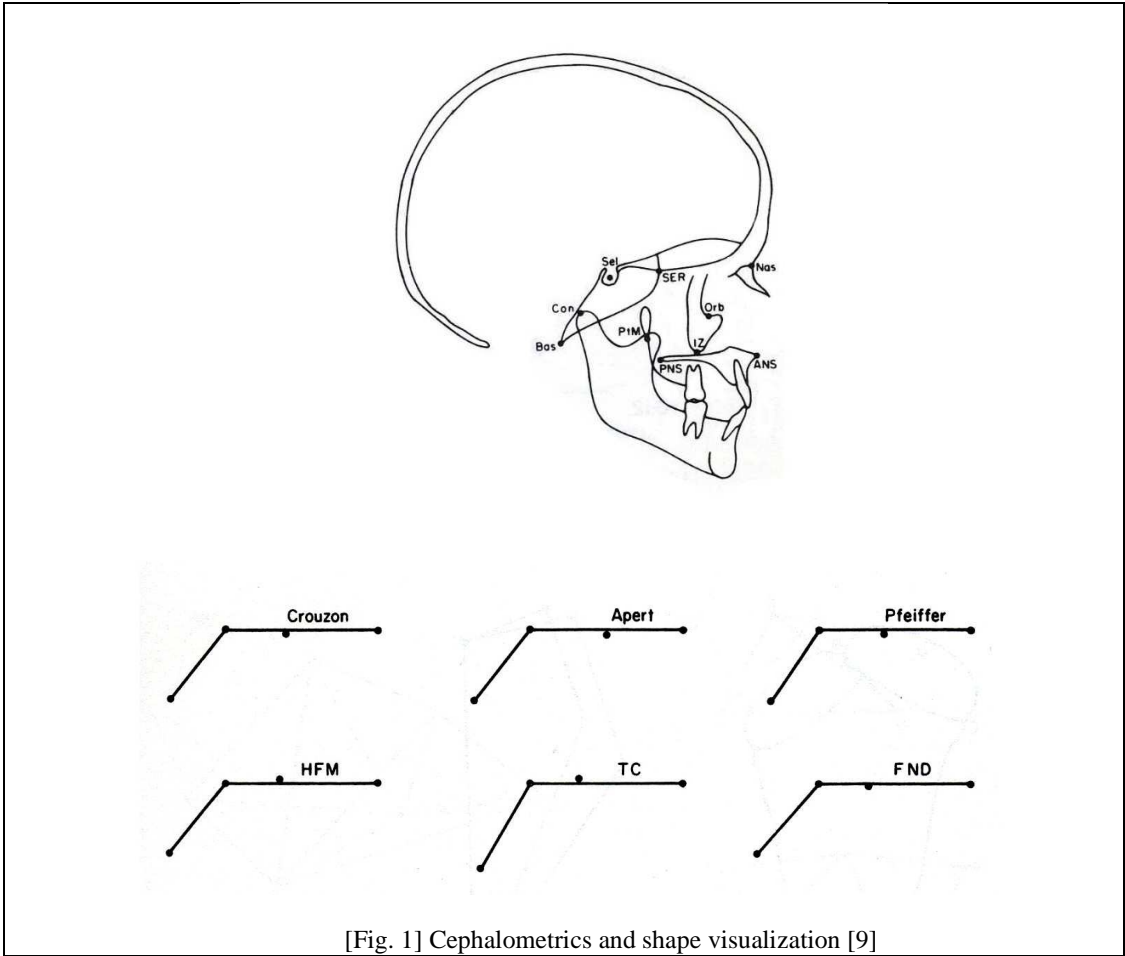
[Fig. 1] Cephalometrics and shape visualization [9]
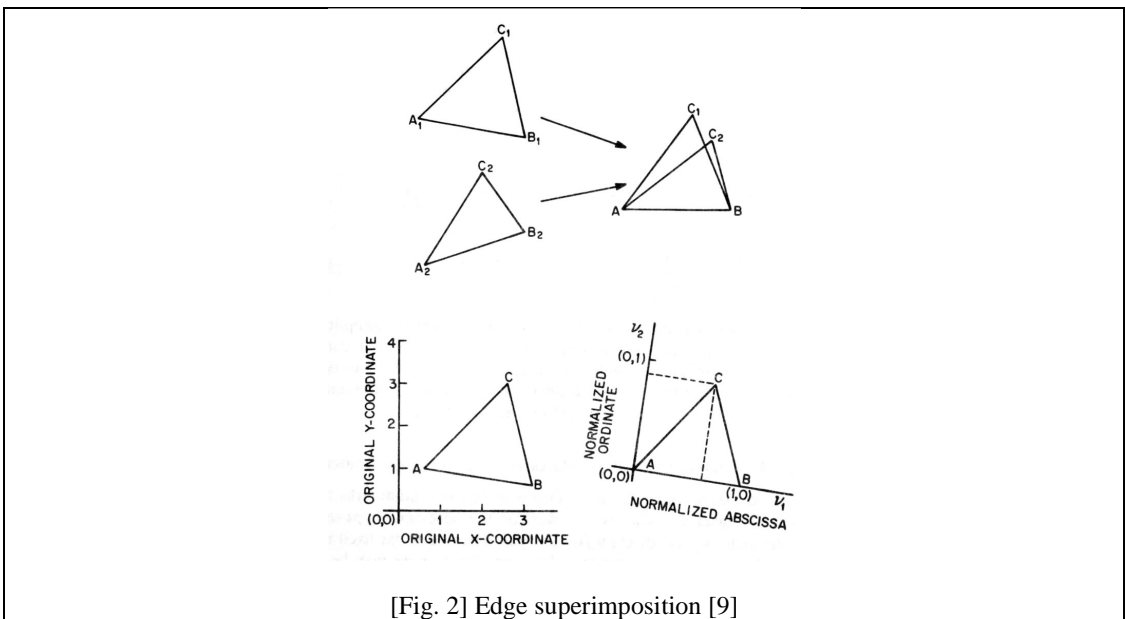
[Fig. 2] Edge superimposition [9]

Since the shape of a geometrical figure is commonly understood to refer to those geometrical attributes that remain unchanged under translation, rotation and scaling, it is preferable to allow realignment of the structure to find the ideal position for comparison.

'Procrustes superimposition' is another type of superimposition that provides an optimum fit and the structure's alignment is free of all arbitrary assumptions beyond the list of landmarks involved[9]. In this method, the geodesics between two shapes are defined and the positioning of the structure is determined by minimizing this distance (Procrustes distance). It allows for direct comparison of shapes and the calculation of the mean[22]. This method has certain advantages, and among them is the fact that multiple specimens of a single population can be superimposed onto a single or base specimen and an average individual for that population can be generated for comparison with others, which also allows intuitive and immediate interpretation [23]. It has been shown in previous studies that Procrustes estimates show no evidence of bias and are the most accurate among the other morphometric methods [24, 25]

. One of the earliest examples of effective use of procrustes method in biologic morphology analysis was a study on the fluctuating asymmetry of the honey bee wings[26]. In this study, several landmarks on honey bee wings were selected and they were aligned in a way defined by procrustes superimposition. The author concluded that this method successfully showed the asymmetric property of the shape, demonstrating a different way of shape analysis than the multivariate analysis or edge superimposition.

1-2.   Current view of craniofacial shape analysis and Previous Studies for a new approach

Conventional cephalometrics has long been used as a standard modality in a variety of circumstances, including studying craniofacial anomalies[27, 28], evaluating growth[29] or treatment outcomes[30, 31], studying dental or skeletal pattern[32, 33], and prediction of surgery[34]. One important application of cephalometrics was obtaining a norm of a certain population, which could then be used for a comparison with other groups of subjects[35]. Despite the overwhelmingly dominant application of cephalometrics a historical review of craniofacial imaging[36] reports the facts limiting the validity of two dimensional cephalometry and its application: 1) A conventional headfilm is a two-dimensional object. 2) It is based on the assumption of a perfect superimposition of the right and left sides. 3) Significant size magnification and distortion errors can result from projection. 4) It has low accuracy and precision. 5) There are landmark identification errors. The unreliability using the landmarks, reference planes, and measurements of 2-dimensional cephalometrics have been documented in a number of studies[37-40].

Recently, the introduction of computed tomography(CT) into the orthodontic specialty has led to the increased application of 3-dimensional data as CT image have shown to provide a more accurate landmark identification and analysis[41-43]. It is documented that CT analysis offers significant advantages and benefits[44, 45] and therefore 3-dimensional analysis has significant potential in diagnosis, treatment planning and outcome evaluation[46].

However, the analyses developed to better understand these images have never fully described 3-dimensional shape, since most of the analyses were repeating the conventional methods used in 2-dimensional radiographs where CT images were only used for linear measurements between conventional cephalometric landmarks [47-54].

These approaches all show the inherent limitations of multivariate morphometrics. The norm that could be obtained using this method is the numerical average of the linear measurements, and the visualization of the shape or its comparison is extremely difficult. Based on these facts, some literature concludes that there is no significant difference in measurements between CT and

conventional cephalograms[55], and that there is no high-quality evidence regarding the benefits of CBCT use in orthodontics[56]. Among the previous researches,a different approach has been shown by a study that incorporated procrustes superimposition to discover the spatial distribution of fifty-two landmarks in 3-dimensional space[57]. A similar methods were used to achieve superimposition and comparison between groups based on ethnicity [24] or gender[58]. In these studies, it was shown that the morphological characteristics of the craniofacial structure can be visualized using numbers of landmarks and the average shapes of groups of subjects could be compared with one another. It should be noted that the number of landmarks were limited in the studies and therefore only the gross outline of the structure could be studied.

One study[59] recently demonstrated the use of procrustes superimposition assisted by the use of topology based registration, to find the normalized surface of sixty-seven skulls. This study showed a great resolution of the surface, revealing the morphologic traits of the craniofacial structure of an individual or a group of individuals.
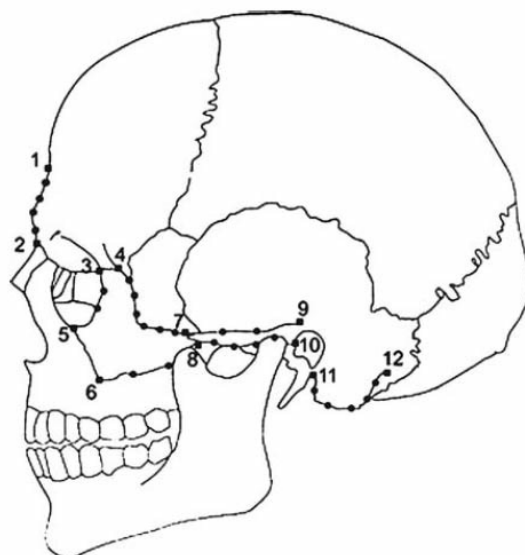
[Fig.3] Superimposition of the craniofacial landmarks without using cranial base[58]

A more accurate outline of anatomical structures can be the described using continuous curves approximated by a larger number of landmarks and pseudo-landmarks along the structure. This approach was used to delineate the 2-dimensional image of the human mandible successfully showing a direct morphologic comparison between the average of a treatment group and control group[60]. A similar method was expanded into 3-dimensions where average shapes were obtained for different developmental stages of a rabbit orbit and differences in size and shape were investigated[61]. In both of these studies, fourier analysis provided a set of functions that led to a smooth and continuous curve connecting the points. Most recently, there was an attempt to use the same method to describe the human mandible with 104 points collected along the border of the image and to find the average of 10 subjects [62]. Although rotational alignment was not corrected for the samples, procrustes superimposition allowed the comparison of shapes under the best fit found by repositioning the structure along three axes, which has been presented in a visualized way. This study on the human mandible has proven the possibility that the 3-dimensional craniofacial structure can be represented by curved outlines defined by a number of point coordinates, allowing normalization and superimposition.

[Fig. 4] Outline of the Mandible and the normalization of ten samples[62]
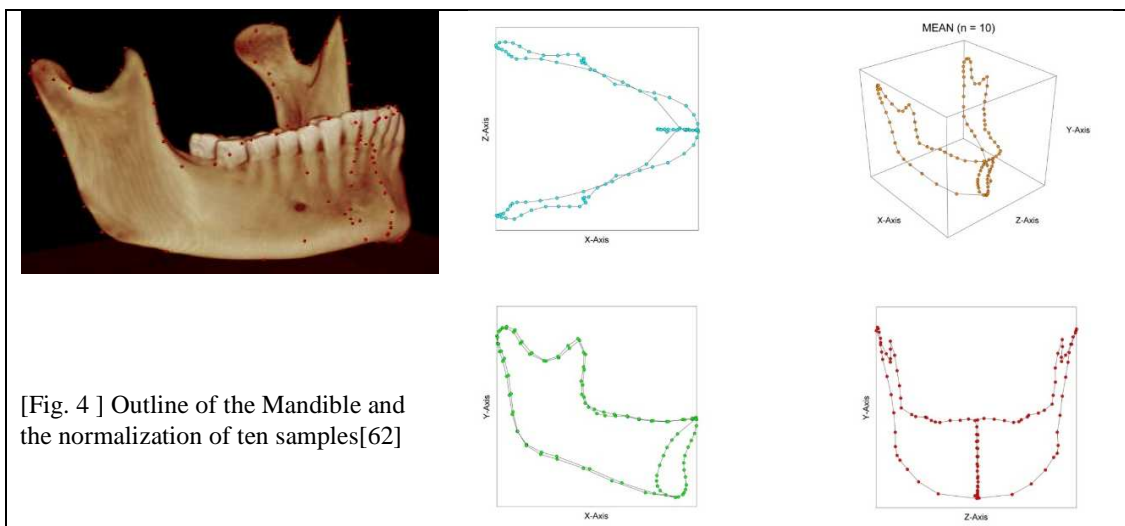
Traditionally, craniofacial structures were divided into three major parts – cranium, maxilla, and mandible - since they are distinct in their features and growth patterns[63]. The final shape representation of the craniofacial structure should include all three components.

The aim of this study is to develop a way to represent the shape of the maxilla, mandible and cranial base-zygoma which will allow superimposition, comparison, and normalization of the components as well as the entire facial complex. To overcome the shortcomings of conventional cephalometrics and provide a useful application, it can be summarized that this new approach must :

1. Avoid excessive dependence on limited landmarks

2. Represent the actual shape

3. Allow Superimposition

4. Provide Normal(Average) form

5. Allow Statistical results for comparison

The new approach will allow a true 3-dimensional morphometric method for analyzing craniofacial structure, which will serve as a basis for more reliable diagnostic and analytic tools.

2. Materials and Methods

2-1.   Collection of the coordinate information

CBCT images taken at the UCLA School of Dentistry by the Newtom 5G CBCT scanner (Image Works) were collected. This will include patients that are candidates for Orthodontic treatment, as well as patients from other departments at UCLA such as OMFS, Periodontics, and Orofacial pain. Images were imported into a beta version of Dolphin Imaging ® software for initial analysis. Following image import, the samples with significant craniofacial defects were excluded, resulting in a collection of 10 samples in total without morphologic abnormality. All the subjects were females, between age of 19 to 37 at the time the images were taken. The image was formatted for optimum hard tissue threshold of opacity. Finally, the 3-dimensional image was sectioned out according to five different specific regions of interest for the purpose of defining the outline of the mandible, maxilla and cranial base (Fig. 5). Using an interface developed for a previous study[62], point coordinates were collected for each structure where all the measurements were made in millimeters. The collection of coordinates was divided into three different components, resulting in a total of 104 points, 92 points, and 117 points for Mandible, Maxilla and Cranial base / zygoma , repectively.

The coordinate data for each component was saved as a text file (Table 1, 2, 3), ready to be used for the following geometric realignment and analysis.

1	Frontal	165.1	44.0	50.5
2	RFrontal	156.2	43.6	50.6
3	RFrontal -1	146.4	45.8	50.4
4	RFrontal -2	136.4	48.0	49.6
5	RFrontal -3	126.9	52.3	48.7
6	RFrontal -4	118.9	59.1	47.0
7	RTemporal	115.9	59.4	42.3
8	RTemporal -1	113.4	62.3	34.7
9	ROutZygoFront	112.3	66.3	28.2
10	ROutZygoFront -1	110.7	69.5	25.0
11	ROutZygoFront -2	111.3	69.5	20.5
12	ROutZygoFront -3	112.0	70.5	15.8
13	RUpZygoma	111.2	73.1	12.3
14	RUpZygoma -1	107.6	79.6	9.2
15	RUpZygoma -2	105.1	85.4	8.8
16	RUpZygoma -3	102.3	95.5	7.3
17	RUpZygoma -4	102.3	100.3	7.1
18	RUpZygoma -5	105.2	114.4	7.4
19	RLowZygoma	107.9	116.4	4.2
20	RLowZygoma -1	106.8	107.7	6.9
21	RLowZygoma -2	104.1	104.7	2.5
22	RLowZygoma -3	104.8	96.8	3.6
23	RLowZygoma -4	105.2	90.6	4.2
24	RLowZygoma -5	106.6	85.6	3.5
25	RLowZygoma -6	108.9	79.9	0.9
26	RLowZygoma -7	111.7	76.3	-1.0
27	RLowZygoma -8	115.7	73.1	-6.0
28	RLowZygoma -9	119.1	70.9	-7.8
29	RKeyridge	123.5	67.4	-9.2
30	RZygoMax -3	124.6	63.7	-4.9
31	RZygoMax -2	126.6	61.6	-0.1
32	RZygoMax -1	128.2	59.6	3.9
33	RZygoMax	127.8	56.9	7.9
34	RLatOrbit	122.1	60.5	12.7
35	RLatOrbit -1	118.8	62.7	18.5
36	RLatOrbit -2	117.8	63.4	24.0
37	RInZygoFront	117.2	60.1	32.7
38	RInZygoFront -1	120.4	55.2	38.5
39	RInZygoFront -2	127.8	51.9	42.6
40	RInZygoFront -3	136.0	49.8	44.6
41	RInZygoFront -4	144.7	48.0	45.3
42	RInZygoFront -5	152.9	46.6	42.0
43	FrontoNasal	156.6	49.8	36.8
44	FrontoNasal -1	160.7	46.2	39.5
45	Nasion	165.4	45.0	41.5
46	Frontal	165.1	44.0	50.5
47	LFrontal	173.1	44.0	51.9
48	LFrontal -1	180.9	45.4	52.4

49	LFrontal -2	189.5	47.9	52.2
50	LFrontal -3	198.2	51.5	52.4
51	LFrontal -4	204.3	55.5	52.0
52	LTemporal	210.2	60.9	51.2
53	LTemporal -1	213.5	58.7	43.7
54	LOutZygoFront	216.3	63.1	38.2
55	LOutZygoFront -1	218.8	69.5	31.9
56	LOutZygoFront -2	218.8	71.3	26.5
57	LOutZygoFront -3	219.1	70.9	22.1
58	LUpZygoma	219.2	72.2	18.6
59	LUpZygoma -1	221.0	76.3	14.0
60	LUpZygoma -2	224.7	84.3	12.7
61	LUpZygoma -3	228.2	93.9	11.9
62	LUpZygoma -4	229.3	103.2	10.9
63	LUpZygoma -5	225.3	115.1	12.7
64	LLowZygoma	227.5	123.9	13.9
65	LLowZygoma -1	220.8	123.1	6.0
66	LLowZygoma -2	224.5	116.0	7.2
67	LLowZygoma -3	227.8	106.3	5.2
68	LLowZygoma -4	227.6	100.7	5.7
69	LLowZygoma -5	226.4	96.4	7.8
70	LLowZygoma -6	225.6	87.4	8.5
71	LLowZygoma -7	223.2	82.6	5.3
72	LLowZygoma -8	220.3	78.7	1.2
73	LLowZygoma -9	217.6	75.3	-2.1
74	LKeyridge	212.9	69.9	-5.5
75	LZygoMax -3	213.5	67.4	1.4
76	LZygoMax -2	212.7	65.1	6.0
77	LZygoMax -1	211.2	61.6	10.1
78	LZygoMax	208.6	59.5	13.3
79	LLatOrbit	211.0	62.3	18.4
80	LLatOrbit -1	212.6	63.7	24.6
81	LLatOrbit -2	213.1	62.9	31.1
82	LInZygoFront	213.0	60.5	36.0
83	LInZygoFront -1	207.8	55.1	41.7
84	LInZygoFront -2	200.9	51.8	45.1
85	LInZygoFront -3	191.3	49.0	46.4
86	LInZygoFront -4	181.4	50.8	45.2
87	LInZygoFront -5	175.4	46.8	42.4
88	FrontoNasal	175.1	51.5	36.6
89	FrontoNasal -1	169.8	46.4	38.8
90	Nasion	165.4	45.0	41.5
91	Frontal	165.1	44.0	50.5
92	Cranial	164.5	59.8	52.8
93	Cranial -1	164.6	63.7	48.6
94	Cranial -2	165.2	67.0	42.4
95	Cranial -3	165.3	70.8	37.1
96	UpEthmoid	163.8	84.6	31.9
97	UpEthmoid -1	163.7	89.3	31.2
98	UpEthmoid -2	163.5	93.7	30.9
99	UpEthmoid -3	162.8	97.7	33.3

100 UPEthmoid -4	163.9	102.1	31.8
101 Sella	164.4	105.4	29.9
102 Sella -1	163.6	106.6	28.2
103 Sella -2	164.0	107.6	23.4
104 Sella -3	164.6	109.6	22.4
105 Sella -4	165.7	112.7	21.0
106 Sella -5	163.9	114.8	29.4
107 PostCranial	164.0	116.3	27.4
108 PostCranial -1	164.2	116.6	22.1
109 PostCranial -2	165.1	117.7	14.3
110 PostCranial -3	166.0	122.0	-0.1
111 Basion	166.6	126.3	-15.6
112 LowEthmoid	167.4	112.7	-2.7
113 LowEthmoid -1	165.9	102.6	-0.3
114 LowEthmoid -2	164.9	89.6	5.4
115 LowEthmoid -3	164.5	81.4	13.5
116 LowEthmoid -4	163.6	83.9	22.6
117 UpEthmoid	163.8	84.6	31.9

[Table 1] Point coordinate text file of subject 1 (Cranial Base / Zygoma)

1	RInfOrbitalrim	155.7	50.8	36.7
2	RInfOrbitalrim -1	157.3	53.4	31.0
3	RInfOrbitalrim -2	157.3	53.1	26.1
4	RInfOrbitalrim -3	156.3	52.6	20.9
5	RInfOrbitalrim -4	153.0	52.9	16.9
6	RInfOrbitalrim -5	149.1	53.4	14.1
7	RInfOrbitalrim -6	143.9	53.7	12.1
8	RInfOrbitalrim -7	138.8	54.0	9.9
9	ROrbitale	132.8	55.2	8.5
10	RZygoMax	127.8	56.9	7.9
11	RZygoMax -1	128.2	59.6	3.9
12	RZygoMax -2	126.6	61.6	-0.1
13	RZygoMax -3	124.6	63.7	-4.9
14	RKeyridge	123.5	67.4	-9.2
15	RKeyridge -1	128.8	68.8	-10.5
16	RKeyridge -2	134.1	66.8	-13.5
17	RKeyridge -3	138.3	66.9	-16.2
18	RKeyridge -4	141.2	65.9	-20.5
19	RKeyridge -5	142.5	64.9	-26.4
20	RU6	141.9	63.6	-32.9
21	RU6-1	144.2	58.6	-34.8
22	RU6-2	144.7	51.5	-36.2
23	RU6-3	147.6	47.9	-35.9

24	RU6-4	150.4	44.0	-35.0
25	RU6-5	156.7	41.1	-34.1
26	RU6-6	40.2	-35.0	
27	Uppermid	168.6	39.6	-35.1
28	LabialCEJ	168.8	41.1	-26.2
29	A-point	168.2	42.9	-19.3
30	ANS	168.5	44.0	-9.8
31	ANS -1	164.0	46.5	-9.3
32	ANS -2	159.8	49.4	-9.3
33	ANS -3	50.8	-4.0	
34	RPiriform	154.8	50.8	1.5
35	RPiriform -1	155.3	49.3	7.4
36	RPiriform -2	156.5	48.0	12.5
37	RPiriform -3	158.8	50.3	18.7
38	RPiriform -4	160.2	50.4	24.1
39	RPiriform -5	160.5	51.5	28.0
40	RPiriform -6	160.2	49.3	34.1
41	RInfOrbitalrim	155.7	50.8	36.7
42	LInfOrbitalrim	175.3	54.2	34.2
43	LInfOrbitalrim -1	173.8	52.2	27.8
44	LInfOrbitalrim -2	174.5	51.5	23.5
45	LInfOrbitalrim -3	177.4	51.6	19.0
46	LInfOrbitalrim -4	181.4	53.0	16.2
47	LInfOrbitalrim -5	188.6	53.0	13.4
48	LInfOrbitalrim -6	193.7	54.1	12.2
49	LInfOrbitalrim -7	199.1	55.8	11.7
50	LOrbitale	203.9	57.6	12.0
51	LZygoMax	208.6	59.5	13.3
52	LZygoMax -1	211.2	61.6	10.1
53	LZygoMax -2	212.7	65.1	6.0
54	LZygoMax -3	213.5	67.4	1.4
55	LKeyridge	212.9	69.9	-5.5
56	LKeyridge -1	208.1	70.0	-7.5
57	LKeyridge -2	200.1	68.1	-11.1
58	LKeyridge -3	196.2	68.7	-15.1
59	LKeyridge -4	194.5	67.4	-22.6
60	LKeyridge -5	197.6	61.7	-33.3
61	LU6	192.8	58.4	-32.7
62	LU6 -1	191.1	51.7	-33.2
63	LU6 -2	188.6	48.3	-32.7
64	LU6 -3	184.8	44.6	-32.6
65	LU6 -4	180.5	41.8	-33.6
66	LU6 -5	175.1	40.0	-34.2
67	LU6 -6	169.8	39.6	-35.4
68	Uppermid	168.6	39.6	-35.1
69	LabialCEJ	168.8	41.1	-26.2
70	A-point	168.2	42.9	-19.3
71	ANS	168.5	44.0	-9.8
72	ANS -1	176.5	50.1	-9.5
73	ANS -2	178.6	51.2	-6.3
74	ANS -3	179.0	50.4	-1.4

75	LPiriform	178.7	49.3	5.0
76	LPiriform -1	177.8	47.5	11.4
77	LPiriform -2	175.8	49.3	15.3
78	LPiriform -3	173.0	48.2	19.9
79	LPiriform -4	170.6	49.3	25.9
80	LPiriform -5	170.0	50.4	29.8
81	LPiriform -6	169.7	48.2	35.9
82	LInfOrbitalrim	175.3	54.2	34.2
83	ANS	168.5	44.0	-9.8
84	Palate	165.6	58.8	-0.7
85	IncisCan	167.1	62.0	-7.9
86	IncisCan -1	166.4	74.9	-6.6
87	PNS	166.9	89.2	-13.3
88	PNS -1	168.2	72.4	-11.7
89	PalatalRidge	167.0	62.6	-13.2
90	PalatalRidge -1	166.8	57.4	-16.8
91	PalatalCEJ	168.0	51.5	-24.6
92	Uppermid	168.6	39.6	-35.1

[Table 2] Point coordinate text file of subject 1 (Maxilla)

1	RtTopCondyle	110.5	113.6	6.0
2	RtTopCondyle -1	113.9	110.5	6.6
3	RtTopCondyle -2	112.7	108.9	4.5
4	RtTopCondyle -3	110.2	107.7	-2.3
5	RtCorNotch	118.8	97.1	-11.1
6	RtCorNotch -1	118.9	87.9	-5.0
7	RtCorNotch -2	118.2	86.6	-1.3
8	RtCorTip	118.5	84.9	0.2
9	RtCorTip -1	119.9	83.2	-1.0
10	RtCorTip -2	121.8	84.2	-10.2
11	RtCorTip -3	124.5	85.0	-16.7
12	RtCorTip -4	125.7	85.0	-23.1
13	RtAlvBorder	127.9	84.6	-29.1
14	RtAlvBorder -1	132.1	86.1	-34.4
15	RtAlvBorder -2	140.4	74.1	-35.7
16	DistalLR6	144.1	69.6	-34.9
17	DistalLR6 -1	147.8	64.9	-33.4
18	MesialLR6	150.3	62.7	-35.0
19	MesialLR6 -1	152.1	58.9	-35.2
20	MesialLR6 -2	153.4	52.9	-33.7
21	LR3Tip	156.4	47.4	-33.4
22	LR3Tip -1	160.7	45.0	-33.5
23	LR3Tip -2	164.4	44.3	-32.9

24	DentMidline	168.9	43.2	-32.6
25	DentMidline -1	169.0	42.5	-36.2
26	CEJ	169.3	43.2	-39.5
27	CEJ -1	169.6	44.3	-44.3
28	CEJ -2	169.6	46.0	-47.7
29	B-point	169.8	46.5	-52.1
30	B-point -1	169.8	46.1	-55.8
31	B-point -2	169.9	45.7	-58.7
32	B-point -3	169.5	45.0	-61.4
33	Pog	170.3	44.0	-65.0
34	Pog -1	170.5	43.9	-66.1
35	Pog -2	170.5	44.3	-67.2
36	Pog -3	170.9	44.7	-68.1
37	Me	170.7	46.9	-70.5
38	Me -1	183.5	51.7	-70.0
39	Me -2	197.2	66.3	-65.1
40	Me -3	205.9	81.0	-56.7
41	LtAntGonNotch	209.4	93.8	-51.7
42	LtAntGonNotch -1	210.2	98.4	-53.2
43	LtGonAngle	211.3	106.2	-49.6
44	LtGonAngle -1	211.3	109.9	-46.0
45	LtGonAngle -2	211.6	112.4	-39.3
46	LtGonAngle -3	213.1	112.0	-29.3
47	LtGonAngle -4	214.9	112.5	-20.9
48	LtConNeck	218.1	113.0	-12.6
49	LtConNeck -1	219.6	116.0	-8.1
50	LtConNeck -2	220.7	118.1	-4.2
51	LtConNeck -3	217.7	119.1	1.6
52	LtConNeck -4	216.8	117.5	8.1
53	LtTopCondyle	215.6	114.0	8.4
54	LtTopCondyle -1	220.6	109.4	5.1
55	LtTopCondyle -2	221.1	109.1	-2.2
56	LtTopCondyle -3	214.7	106.2	-6.4
57	LtCorNotch	212.7	100.9	-10.1
58	LtCorNotch -1	213.1	96.2	-6.1
59	LtCorNotch -2	212.7	93.0	-2.2
60	LtCorTip	211.0	88.9	3.5
61	LtCorTip -1	210.4	88.3	0.3
62	LtCorTip -2	209.5	88.9	-7.5
63	LtCorTip -3	209.0	89.7	-15.2
64	LtCorTip -4	207.3	89.3	-20.5
65	LtAlvBorder	205.6	89.3	-25.2
66	LtAlvBorder -1	195.4	78.1	-30.9
67	LtAlvBorder -2	193.1	74.8	-31.3
68	DistalLL6	190.9	71.6	-31.8
69	DistalLL6 -1	190.2	66.8	-31.3
70	MesialLL6	187.3	63.7	-33.8
71	MesialLL6 -1	186.3	59.3	-31.8
72	MesialLL6 -2	184.6	54.1	-32.5
73	LL3Tip	182.5	48.1	-32.1
74	LL3Tip -1	177.9	46.1	-32.2

75	LL3Tip -2	172.5	45.1	-31.9
76	DentMidline	168.9	43.2	-32.6
77	CEJLingual	169.6	49.6	-38.1
78	CEJLingual -1	170.0	49.6	-41.1
79	CEJLingual -2	170.0	52.1	-43.8
80	CEJLingual -3	170.0	52.8	-46.2
81	CEJLingual -4	170.0	53.2	-48.7
82	ConcavePtChin	170.1	54.3	-53.0
83	ConcavePtChin -1	170.0	55.4	-57.8
84	ConcavePtChin -2	170.1	55.4	-62.1
85	ConcavePtChin -3	170.2	55.0	-64.8
86	ConcavePtChin -4	170.4	53.9	-67.3
87	Me	170.7	46.9	-70.5
88	RtMe -1	161.6	54.7	-71.6
89	RtMe -2	146.6	61.1	-69.4
90	RtMe -3	136.1	71.1	-63.5
91	RtAntGonNotch	127.1	89.6	-56.7
92	RtAntGonNotch -1	124.3	96.8	-56.0
93	RtGonAngle	122.4	101.7	-54.9
94	RtGonAngle -1	121.3	104.8	-50.4
95	RtGonAngle -2	121.7	108.7	-44.2
96	RtGonAngle -3	119.2	108.2	-34.1
97	RtGonAngle -4	115.9	109.3	-24.9
98	RtConNeck	112.7	110.9	-16.0
99	RtConNeck -1	109.8	111.9	-12.5
100	RtConNeck -2	107.7	113.4	-8.6
101	RtConNeck -3	106.5	114.9	-4.4
102	RtConNeck -4	106.2	114.8	-0.9
103	RtConNeck -5	108.4	115.3	2.8
104	RtTopCondyle	110.5	113.6	6.0

[Table 3] Point coordinate text file of subject 1 (Mandible)

[Fig. 5] A screen capture of collecting points
(A) Subject 1 (B) Right Zygoma (C) Left Zygoma (D) Mid Cranial Base (E) Right Maxilla (F) Left Maxilla
(G) Palate (H) Mandible
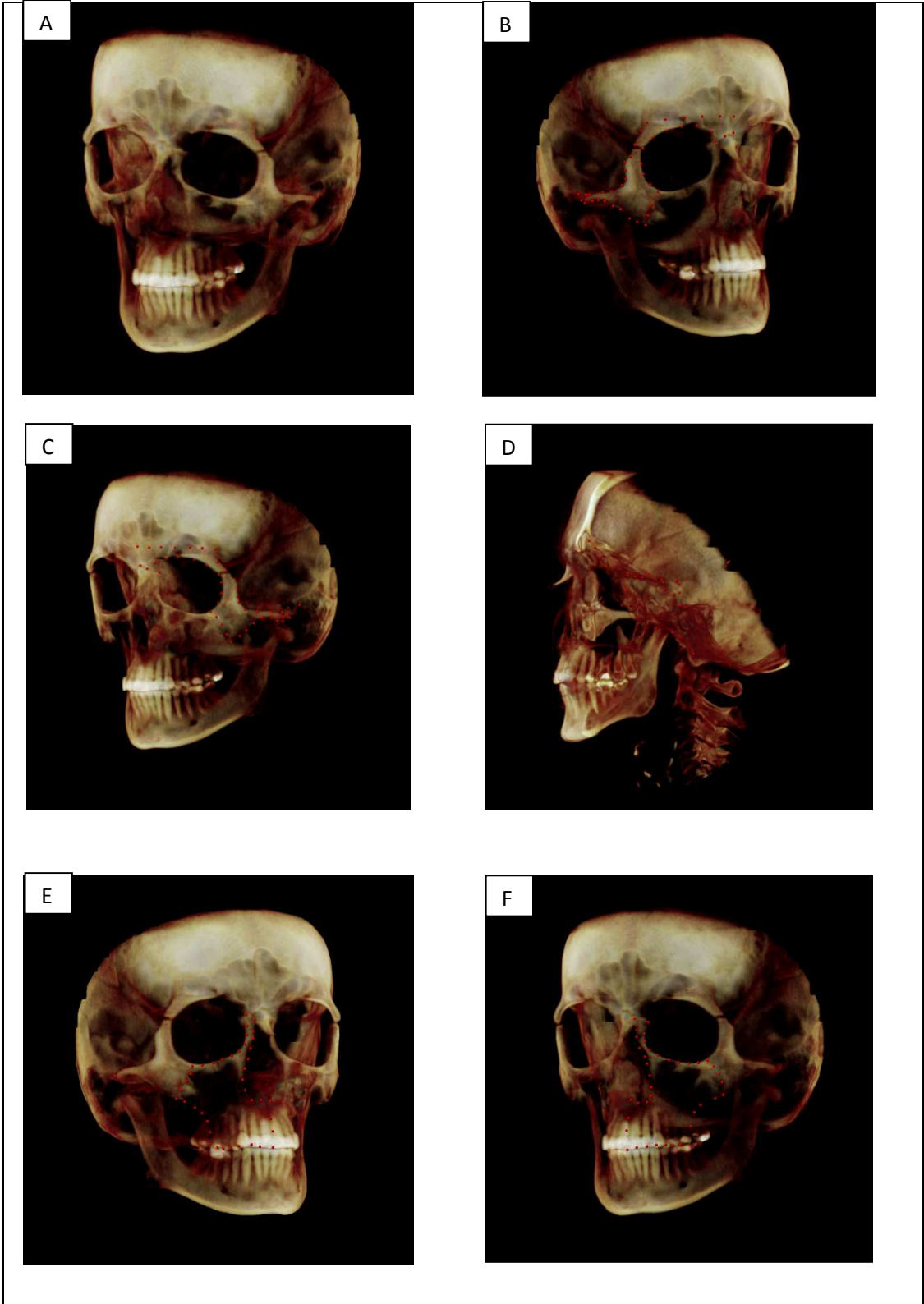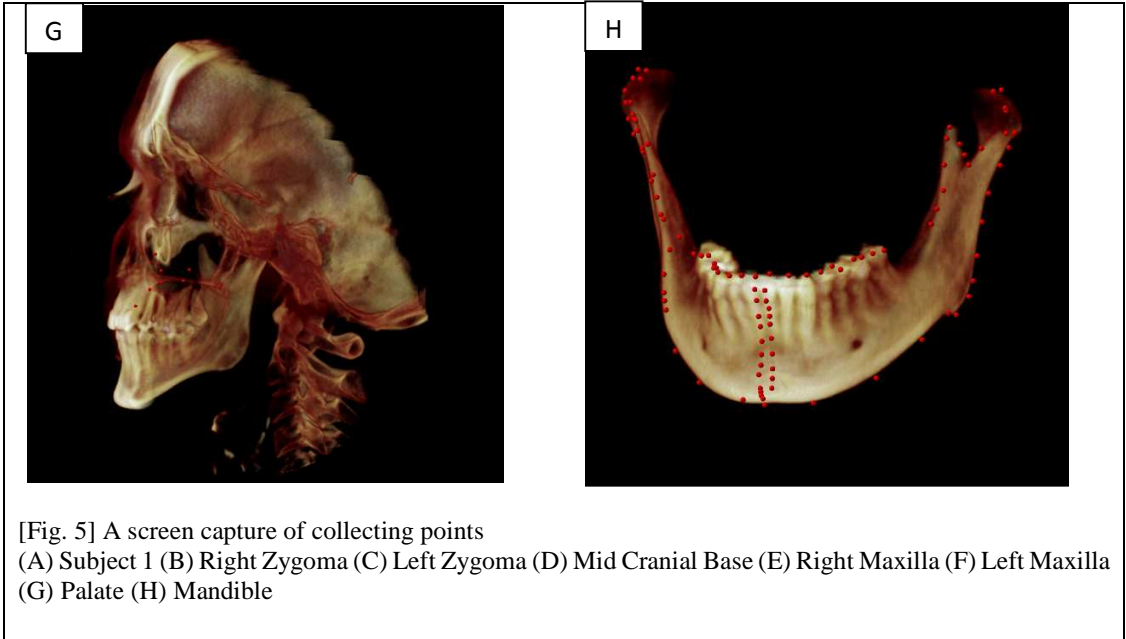
2-2. Shape registration and alignment of each component

Correspondence of points in each component was assumed based on manual labeling as shown in the previous example of the text file for the mandible. Methods for automated curve registration exist; however, we found that the original manually-defined correspondence appears at least as accurate and often more accurate than results from some state-of-the-art curve registration approaches.

Given a pair of homologous weighted point sets $\{x_i, y_i, w_i\}, x_i, y_i \in \mathbb{R}^3, w_i \in \mathbb{R}$, the transformation that minimizes the sum of squared distances between each pair of points is known as a Procrustes alignment [64], and can be encoded by a 4x4 homogenous matrix A. This matrix minimizes the following functional:

$$C(A) = \sum_i w_i (A\tilde{x_i} - \tilde{y_i})^2, \tag{1}$$

where $\widetilde{x_i}, \widetilde{y_i}$ are the 4-dimensional versions of the original point sets, augmented by 1 in the 4th dimension to account for translation.

2-3.   Computing Average Affine Transformations

Assuming existing correspondence, we seek an average position, size, and orientation – the mean affine transformation – of the average shape, given the sample of normal subjects. It will become clear below why computing the average affine transformation is done prior to computing the average shape itself. In fact, computing the mean transformation is essentially equivalent to computing the average shape itself based on our approximation of the latter.

We note here that a true "average" shape necessitates the idea of a shape metric. In this formalism, shapes can be represented simply as point-sets [9], continuous one-dimensional curves [65], or orientable 2-manifolds [66]. Each of these cases leads to a different metric formulation, $d: \mathcal{M} \times \mathcal{M} \to \mathbb{R}^+$ forming its own Riemannian manifold of shapes $\mathcal{M}$. In our case, the average shape is approximated simply as the Euclidean average of the individual shapes based on their embedding in the original space R^3, and after removing effects of affine alignment.

A Riemannian metric naturally induces a manifold, and the task of finding a mean of a set of points on this manifold becomes a minimization problem:

$$\bar{A} = \arg\min_A \sum d^2(A, A_i). \tag{2}$$

This is known as the Karcher mean [67]. An equivalent, though more general definition of the Karcher mean is the point whose unit vectors along geodesics to each A_i sum to zero in the tangent space of $\bar{A}$.

While we have tried the formulation of [65], we have found that the Euclidean average approximation with assumed correspondence is most robust. Further, because the essential measurements of interest in clinical practice are based on Euclidean displacement from the norm, such a construction of the normative shape is most appropriate.

The essential idea behind the computation of a mean affine transformation is similar in spirit to the idea of a metric space of shapes. Developed by Roger Woods [68], the approach formulates a semi-Riemannian metric of linear transformations based on matrix exponentiation. As noted in the study [68], the latter definition of the mean can be used to drive a local optimization of (2). This is based on two facts:

1. Given an exponential map on a manifold at point p, or the geodesic path parameterized by t in the direction v, $\gamma_v(t) = \text{Exp}_p(t * v)$, the condition for the mean, $\mathbf{0} = \sum_{j=1}^{N} \text{Exp}_{\bar{A}}^{-1}(A_j)$, is also the local gradient for the current approximation to the mean.

2. As affine transformation matrices form a Lie group, the exponential map on the manifold is equivalent to matrix exponentiation.

This leads to an iterative approach for finding the mean affine transformation.

2-4.   Reconstruction of a comprehensive 3D model

Armed with the computational methods of the previous section, we can now reposition the 1D skull components of each normal subject's the average position. To do this, we can initially choose a single subject to serve as the target for all alignments. In this way, our mean affine transform will be the mean of all inverse transforms to the target. Then, each subject's average repositioning matrix is computed as $A_j * \overline{A^{-1}}$. However, this approach is still potentially

confounded by the arbitrary choice of the target subject, which can reduce the stability of the computed mean. An alternative which avoids this confound is to compute the full set of Nx(N-1) affine alignments, and find the corresponding mean transformation for each subject. This is a true group-wise approach, as no target subject needs to be selected. We use the latter approach, as implemented by Roger Woods in the "AIR Reconcile" program of the AIR package available at http://bishopw.loni.ucla.edu/air5/.

2-5.   Measurements and Analsysis by Superimposition

Two subjects were selected for comparison with the normalized craniofacial complex. First, one subject was internally selected from the original ten subjects. Another subject from a patient with crouzon syndrome was used to represent a specific case that had a great variation from the population used for the normalization. The coordinates of the points that define the boundary were collected for both samples, and procrustes analysis was used to superimpose the cranial base, maxilla, mandible, and the integrated craniofacial complex of each subject with the normalized structures. The deviation from the normalized structure was analyzed in a vector form as well as a linear distance for each landmark. The deviation was also compared with the size-standardized, or non-size-standardized standard deviation internally determined among the original ten samples. The 117, 92, 104, and 313 points for Cranial base, Maxilla, Mandible, and the Craniofacial complex include both sagittal points along the midline and asymmetric points that are off the midline that can be analyzed. All the boundary point data were included in the computation and were analyzed both visually and numerically. Every set of points as morphologic entities and analytic results could be plotted in 3-dimensions using LONI Shapeviewer software® developed by UCLA Laboratory of Neuro-Imaging. However, the

process of reviewing the data will only focus on a limited number of points to simplify the

evaluation. Thus, a number of points was selected as in Table. 4 to represent arbitrary points of

interest.

Components	Type of Landmarks	Points	Description
Cranial Base (CB)	Sagittal	Basion	108th point of Cranial base
		Nasion	45th point of Cranial base
	Asymmetric	Right Fronto-zygomatic	37th point of Cranial base
Maxilla (Mx)	Sagittal	ANS	30th point of Maxilla
		A Point	29th point of Maxilla
	Asymmetric	Rt Orbitale	9th point of Maxilla
		Right Lat. Nasal Cavity	34th opoint of Maxilla
Mandible (Mn)	Sagittal	B point	29th point of Mandible
		Pogonion	33th point of Mandible
		Menton	37th point of Mandible
	Asymmetric	Rt Gonial Angle	93rd point of Mandible
		Rt Condylar Head	1st point of Mandible

[Table 4]   Selected points of interest and the description

3. Results

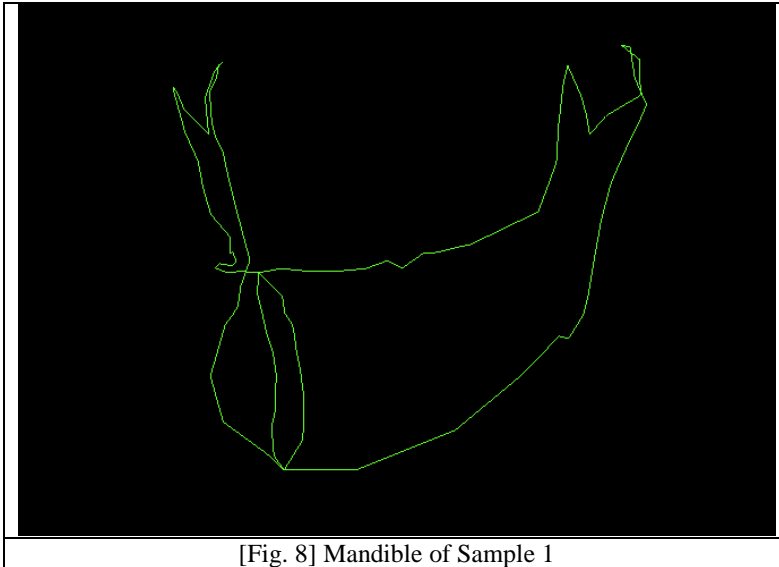## 3-1. Representation of Individual Samples

  The coordinates of the boundary points for the original ten samples showed a well-defined boundary that represents the morphology of each component of each patient. Fig. 6,7,8 Shows an example of one sample.
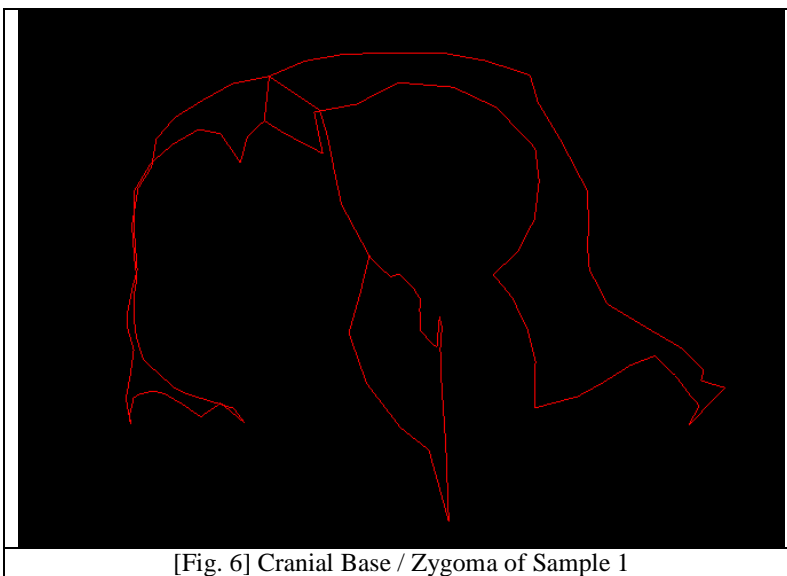

[Fig. 6] Cranial Base / Zygoma of Sample 1

[Fig. 7] Maxilla of Sample 1
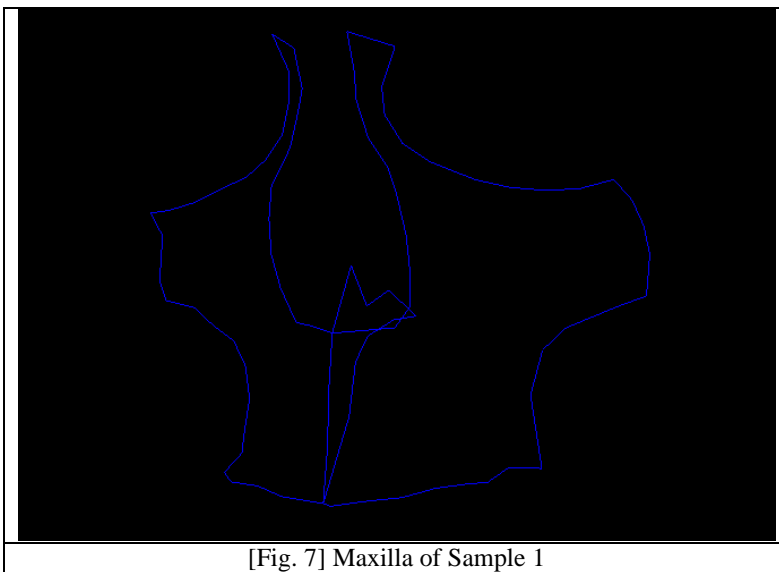
[Fig. 8] Mandible of Sample 1

3-2. Normalized result of each component

10 samples of Cranial base, Maxilla and Mandible respectively are superimposed and averaged to yield a normalized form of each component. Each normalized structure is plotted as shown in Fig. 9,10,11.

The variation within the group of samples was quantified by the deviation of each landmark from one another. Table 5 and Table 6 Show the statistical result of the selected points of each component in the case of non-size-standardization and size-standardization.
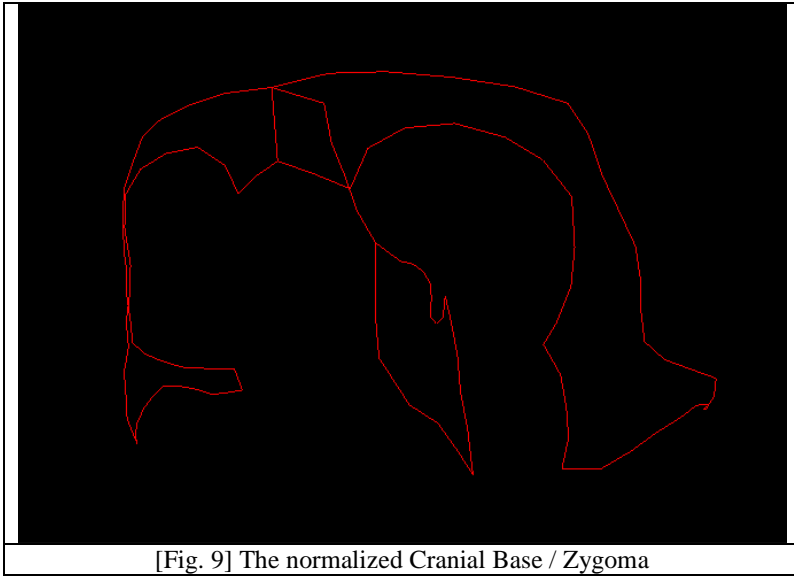
[Fig. 9] The normalized Cranial Base / Zygoma
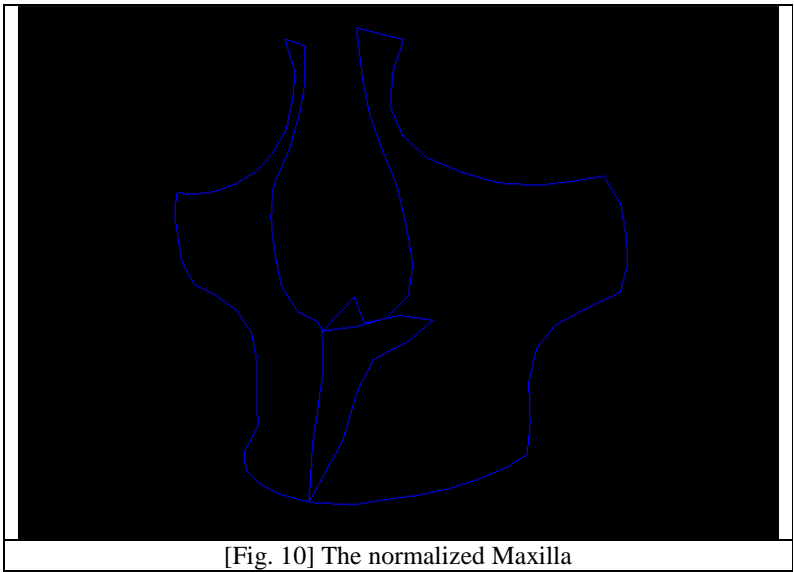
[Fig. 10] The normalized Maxilla

[Fig. 11] The normalized Mandible
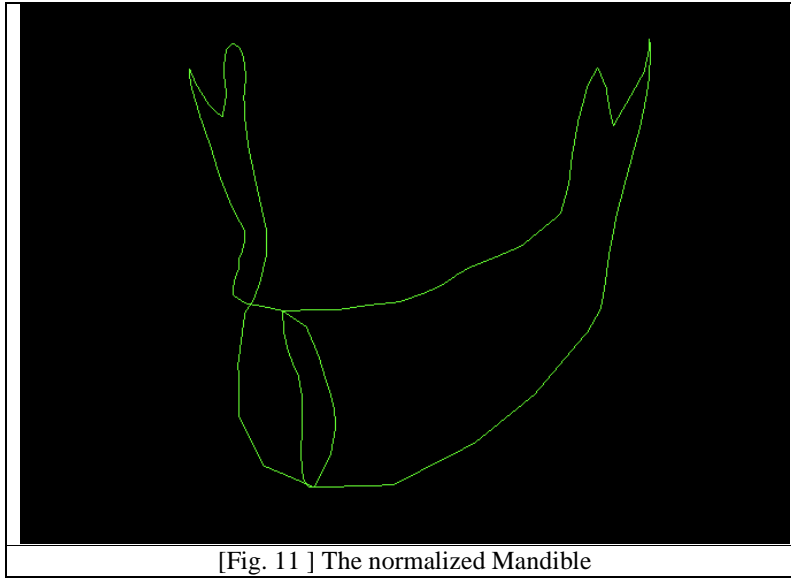
Component	Type of Landmark	Landmark	Non-size-standardized			
			STDV of Coord			STDV of displacement
			x	y	z	
CB	Sagittal	Basion	1.21	2.10	4.32	2.23
		Nasion	0.40	1.39	1.76	1.11
	Asymmetric	Right Fronto-zygomatic	1.97	1.86	1.03	1.51
Mx	Sagittal	ANS	1.10	2.84	1.24	1.52
		A Point	0.93	1.34	1.54	1.05
	Asymmetric	Rt Orbitale	2.73	1.21	1.71	1.47
		Right Lat. Nasal Cavity	0.65	1.39	2.31	1.84
Mn	Sagittal	B point	0.33	1.80	1.54	1.20
		Pogonion	0.56	1.93	2.50	1.96
		Menton	0.63	1.76	1.96	1.60
	Asymmetric	Rt Gonial Angle	2.30	3.93	1.97	2.74
		Rt Condylar Head	3.03	1.02	2.34	2.24

[Table 5] Non-Size-Standardized Result of the Deviation

Component	Type of Landmark	Landmark	Size-standardized			
			STDV of Coord			STDV of displacement
			x	y	z	
CB	Sagittal	Basion	1.18	2.90	4.32	2.44
		Nasion	0.38	1.66	1.70	1.16
	Asymmetric	Right Fronto-zygomatic	0.93	1.38	1.17	0.82
Mx	Sagittal	ANS	1.08	2.99	1.24	1.64
		A Point	0.92	1.50	1.48	1.14
	Asymmetric	Rt Orbitale	2.12	1.23	1.55	1.39
		Right Lat. Nasal Cavity	0.64	1.37	2.27	1.83
Mn	Sagittal	B point	0.34	1.95	1.09	1.11
		Pogonion	0.59	2.04	1.46	1.38
		Menton	0.65	2.00	1.07	1.08
	Asymmetric	Rt Gonial Angle	2.14	3.42	1.98	2.56
		Rt Condylar Head	2.45	1.90	2.59	2.25

[Table 6] Size-Standardized Result of the Deviation

3-3. Average of the complex

Reconstruction of the normalized craniofacial structure was carried out by applying the invert transformation and repositioning each component with respect to one another. The result is a set of 313 points, representing the outline of the normalized craniofacial structure. The normalized feature and numerical values of the coordinates are as shown in Fig. 12 and Table 7.


[Fig. 12] The normalized craniofacial complex
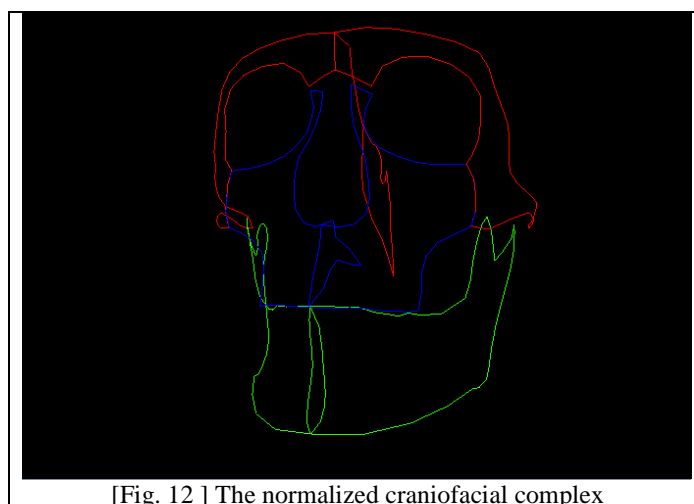
| Component	Type of Landmark	Landmark	Ave Coord		
			x	y	z
CB	Sagittal	Basion	169.44	126.85	31.14
		Nasion	170.63	51.31	58.43
	Asymmetric	Right Fronto-zygomatic	123.95	65.08	52.84
Mx	Sagittal	ANS	170.61	46.98	5.53
		A Point	170.38	47.07	-1.15
	Asymmetric	Rt Orbitale	136.54	58.96	28.22
		Right Lat. Nasal Cavity	157.92	53.39	17.58
Mn	Sagittal	B point	169.45	49.30	-38.35
		Pogonion	169.31	47.56	-52.70
		Menton	169.21	52.01	-58.16
	Asymmetric	Rt Gonial Angle	123.75	112.58	-36.83
		Rt Condylar Head	115.57	121.96	23.49

[Table 7] The normalized coordinate points

3-4. Superimposition of an internal subject with the Norm

The first sample was selected as the internal subject to be superimposed and compared with the norm. The non-size-standardized and size-standardized superimposition of the Cranial base, Maxilla, and Mandible revealed that the coordinates of the boundary points were deviated from the norm, and the visualized comparison is shown in Fig. 13 & 14.
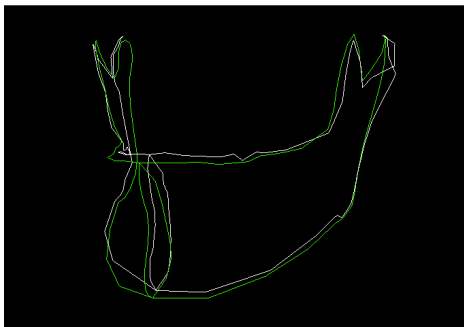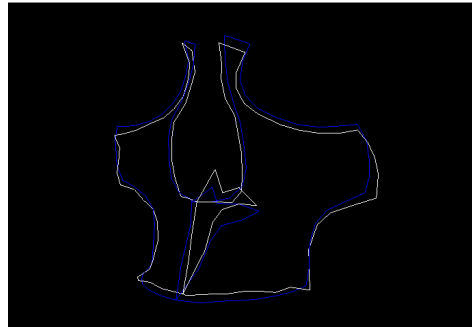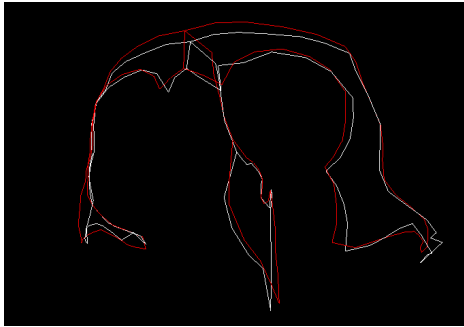
[Fig. 13] Non-Size-Standardized Superimposition of the components of Sample 1

(White: Sample 1, Colored : Norm)
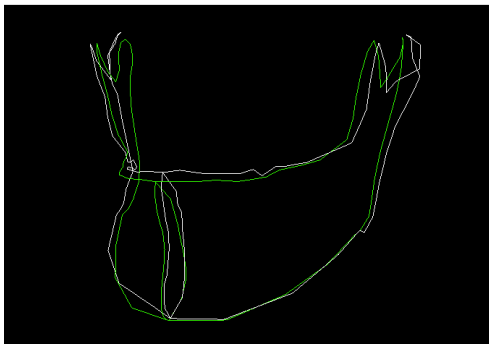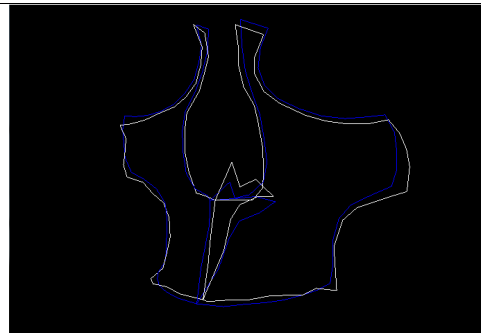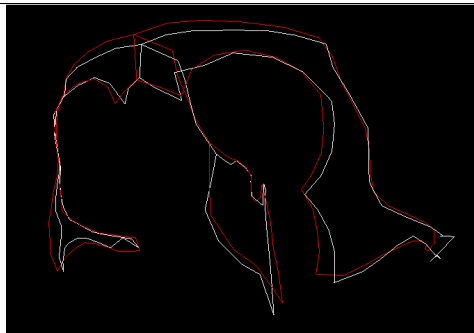
[Fig. 14] Size-Standardized Superimposition of the components of Sample 1

(White: Sample 1, Colored : Norm)

Landmark	Subject Coord.			Deviation of Coord.			Dev. of Coord. In STDV			Dev	Dev. in STDV
	x	y	z	x	y	z	x	y	z		
Basion	168.51	123.42	37.56	-0.93	-3.43	6.42	-0.76	-1.63	1.49	7.33	3.29
Nasion	170.89	52.45	59.04	0.26	1.14	0.60	0.64	0.82	0.34	1.31	1.18
Right Fronto-zygomatic	122.24	67.43	52.96	-1.71	2.35	0.12	-1.71	2.35	0.12	2.91	1.93
ANS	171.76	47.88	5.72	1.14	0.90	0.19	1.04	0.32	0.15	1.47	0.96
A Point	171.07	46.78	-3.76	0.69	-0.28	-2.61	0.74	-0.21	-1.69	2.71	2.59
Right Orbitale	136.53	57.67	25.66	-0.01	-1.28	-2.56	0.00	-1.06	-1.50	2.86	1.94
Rt, Lat. Nasal Cavity	158.34	54.13	17.65	0.42	0.75	0.07	0.64	0.54	0.03	0.86	0.47
B point	169.61	52.58	-37.77	0.16	3.28	0.57	0.50	1.82	0.37	3.33	3.33
Pogonion	169.39	50.19	-50.70	0.07	2.63	2.00	0.13	1.36	0.80	3.31	3.31
Menton	169.54	53.13	-56.19	0.33	1.12	1.97	0.53	0.64	1.00	2.29	2.29
Rt Gonial Angle	123.00	108.51	-37.58	-0.75	-4.07	-0.75	-0.33	-1.03	-0.38	4.20	4.20
Rt Condylar Head	114.54	120.04	23.96	-1.02	-1.93	0.47	-0.34	-1.88	0.20	2.23	2.23

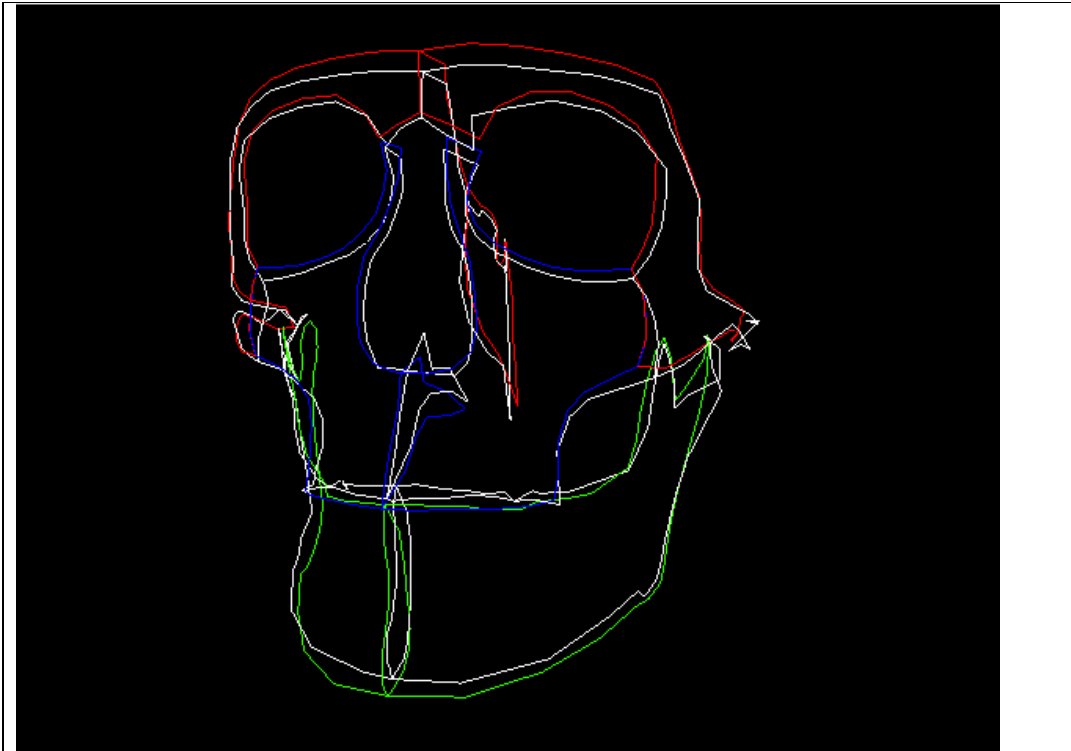[Table 8] Non-Size-standardized superimposition of each component

Numerical values of selected points of the Non-size-standardized superimposition and size-standardized superimposition are given in Table 8 and Table 9.

Landmark	Subject Coord.			Deviation of Coord.			Dev. of Coord. In STDV			Dev	Dev. in STDV
	x	y	z	x	y	z	x	y	z		
Basion	168.50	123.95	37.53	-0.94	-2.90	6.38	0.80	-1.00	1.48	7.07	2.90
Nasion	170.91	52.06	59.28	0.28	0.75	0.85	0.72	0.45	0.50	1.16	1.00
Right Fronto-zygomatic	121.62	67.23	53.13	-2.33	2.15	0.29	-2.50	1.56	0.25	3.18	3.90
ANS	171.78	47.67	5.58	1.17	0.68	0.05	1.08	0.23	0.04	1.36	0.82
A Point	171.08	46.55	-4.10	0.70	-0.52	-2.95	0.76	-0.35	-2.00	3.07	2.71
Right Orbitale	135.80	57.67	25.94	-0.73	-1.29	-2.28	-0.35	-1.05	-1.47	2.72	1.96
Rt, Lat. Nasal Cavity	158.08	54.05	17.77	0.16	0.67	0.18	0.25	0.49	0.08	0.71	0.39
B point	169.67	51.61	-38.42	0.22	2.30	-0.07	0.65	1.18	-0.06	2.31	2.08
Pogonion	169.43	49.14	-51.74	0.12	1.59	0.97	0.21	0.78	0.66	1.86	1.34
Menton	169.59	52.18	-57.40	0.39	0.17	0.77	0.60	0.08	0.72	0.88	0.81
Rt Gonial Angle	121.63	109.25	-38.22	-2.12	-3.33	-1.39	-0.99	-0.97	-0.70	4.19	1.63
Rt Condylar Head	112.92	121.12	25.20	-2.65	-0.85	1.71	-1.08	-0.45	0.66	3.26	1.45

[Table 9] Size-standardized superimposition of each component

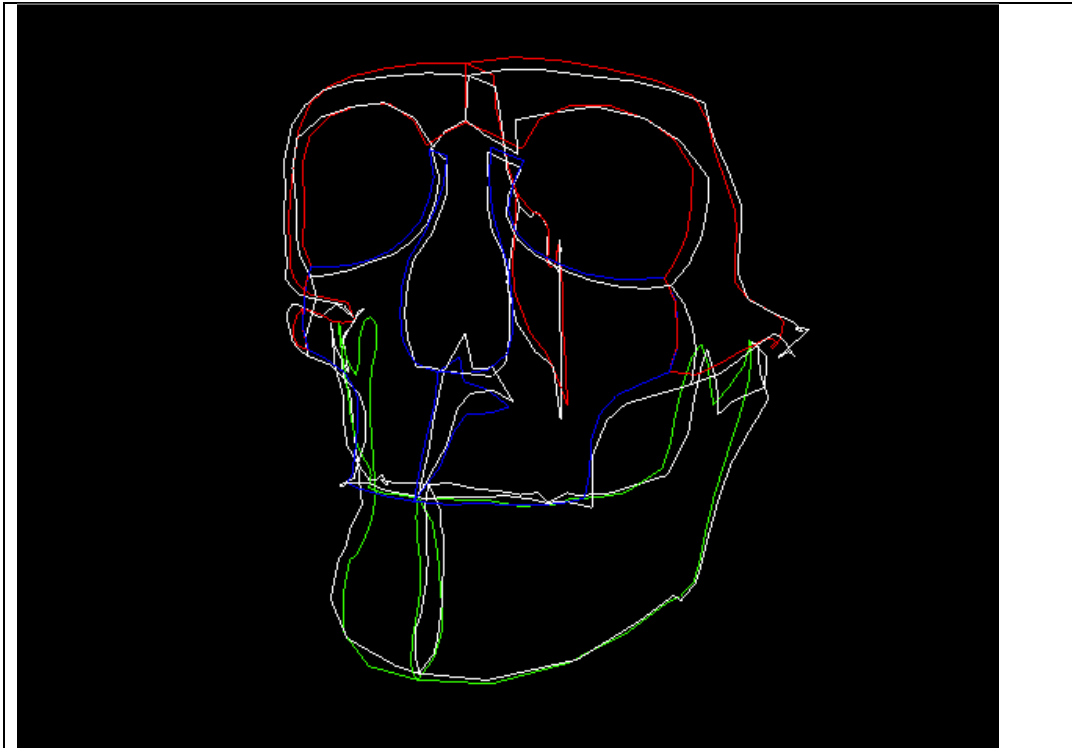The non-size-standardized and size-standardized superimposition can be performed to focus on the overall difference of the craniofacial structures of sample 1 and the normalized form. The visualized result of the superimpositions are provided in Fig. 15 & 16.

[Fig. 15] Non-size-standardized superimposition of the craniofacial complex of Sample 1 with the normalized form

(White : Sample 1 , Colored : Norm)

[Fig. 16] Non-size-standardized superimposition of the craniofacial complex of Sample 1 with the normalized form

Again, selected point data were given in Table 10 and Table 11 for non-size-standardized and size-standardized results.

Landmark	Subject Coord.			Deviation of Coord.			Dev. of Coord. In STDV			Dev	Dev. in STDV
	x	y	z	x	y	z	x	y	z		
Basion	168.72	123.81	38.06	-0.72	-3.04	6.92	-0.61	-1.05	1.60	7.59	3.12
Nasion	170.96	50.45	58.67	0.33	-0.86	0.24	0.85	-0.52	0.14	0.95	0.82
Right Fronto-zygomatic	121.02	65.99	52.32	-2.93	0.90	-0.52	-3.15	0.65	-0.45	3.11	3.81

Landmark	x	y	z	x	y	z	x	y	z	Dev	Dev in STDV
ANS	171.11	48.86	5.87	0.50	1.88	0.35	0.46	0.63	0.28	1.97	1.20
A Point	170.24	47.63	-3.84	-0.14	0.56	-2.69	-0.15	0.38	-1.82	2.75	2.43
Right Orbitale	135.59	60.65	26.63	-0.95	1.70	-1.59	-0.45	1.39	-1.03	2.51	1.81
Rt, Lat. Nasal Cavity	157.74	56.00	18.20	-0.18	2.62	0.61	-0.28	1.91	0.27	2.69	1.47
B point	169.96	50.97	-37.62	0.51	1.67	0.72	1.51	0.86	0.66	1.89	1.70
Pogonion	169.71	48.27	-50.86	0.39	0.71	1.85	0.66	0.35	1.27	2.02	1.46
Menton	169.80	51.19	-56.56	0.59	-0.82	1.61	0.91	-0.41	1.50	1.90	1.76
Rt Gonial Angle	121.27	107.78	-38.30	-2.48	-4.80	-1.47	-1.16	-1.40	-0.74	5.60	2.18
Rt Condylar Head	112.67	120.69	24.75	-2.89	-1.28	1.26	-1.18	-0.67	0.49	3.40	1.52

[Table 10] Non-Size-standardized superimposition of the complex of subject

Landmark	Subject Coord.			Deviation of Coord.			Dev. of Coord. In STDV			Dev	Dev. in STDV
	x	y	z	x	y	z	x	y	z		
Basion	168.72	123.81	38.06	-0.72	-3.04	6.92	-0.61	-1.05	1.60	7.59	3.12
Nasion	170.96	50.45	58.67	0.33	-0.86	0.24	0.85	-0.52	0.14	0.95	0.82
Right Fronto-zygomatic	121.02	65.99	52.32	-2.93	0.90	-0.52	-3.15	0.65	-0.45	3.11	3.81
ANS	171.11	48.86	5.87	0.50	1.88	0.35	0.46	0.63	0.28	1.97	1.20

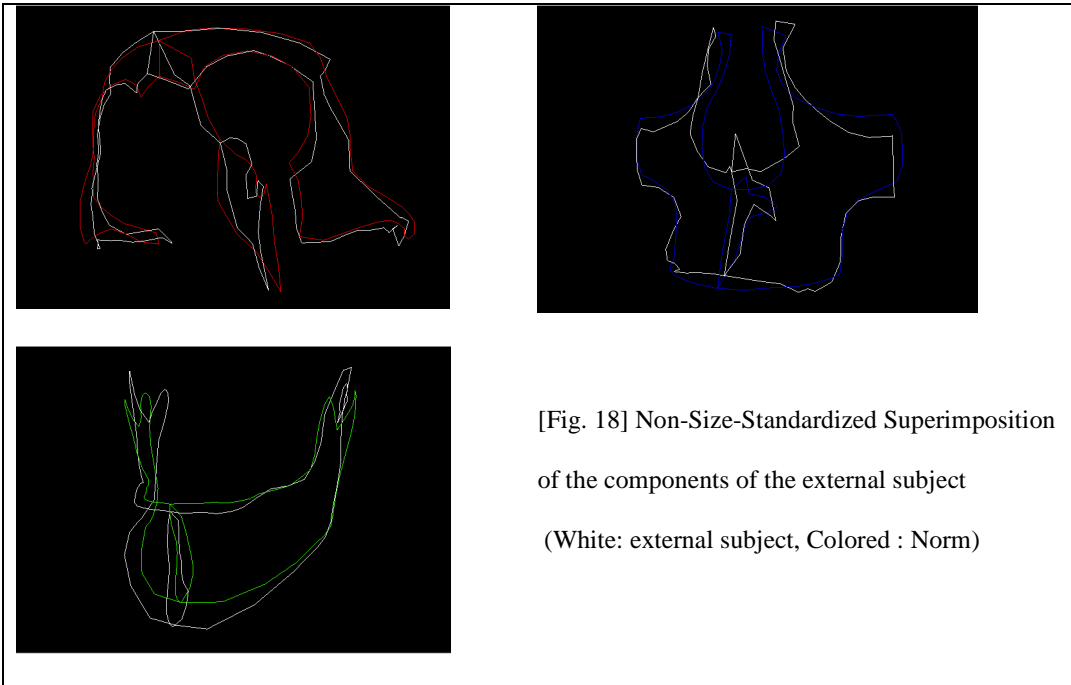|											
A Point	170.24	47.63	-3.84	-0.14	0.56	-2.69	-0.15	0.38	-1.82	2.75	2.43
Right Orbitale	135.59	60.65	26.63	-0.95	1.70	-1.59	-0.45	1.39	-1.03	2.51	1.81
Rt, Lat. Nasal Cavity	157.74	56.00	18.20	-0.18	2.62	0.61	-0.28	1.91	0.27	2.69	1.47
B point	169.96	50.97	-37.62	0.51	1.67	0.72	1.51	0.86	0.66	1.89	1.70
Pogonion	169.71	48.27	-50.86	0.39	0.71	1.85	0.66	0.35	1.27	2.02	1.46
Menton	169.80	51.19	-56.56	0.59	-0.82	1.61	0.91	-0.41	1.50	1.90	1.76
Rt Gonial Angle	121.27	107.78	-38.30	-2.48	-4.80	-1.47	-1.16	-1.40	-0.74	5.60	2.18
Rt Condylar Head	112.67	120.69	24.75	-2.89	-1.28	1.26	-1.18	-0.67	0.49	3.40	1.52

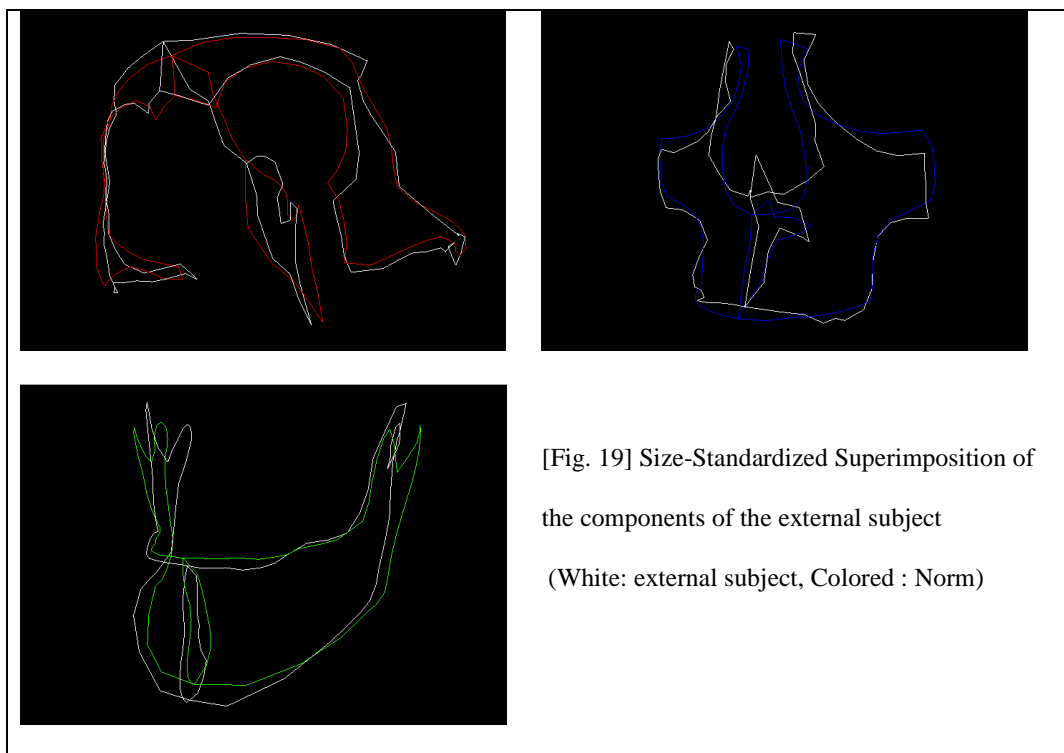[Table 11] Size-standardized superimposition of the complex of subject

3-5. Superimposition of an external subject with the Norm

The boundary information of a CBCT image from a patient diagnosed as Crouzon syndrome (Fig. 17) was collected in the form of point coordinates of Cranial base, Maxilla and Mandible. The set of points was used to be superimposed and compared with the normalized form.

[Fig.17] CBCT image of Crouzon syndrome patient

used as an external subject
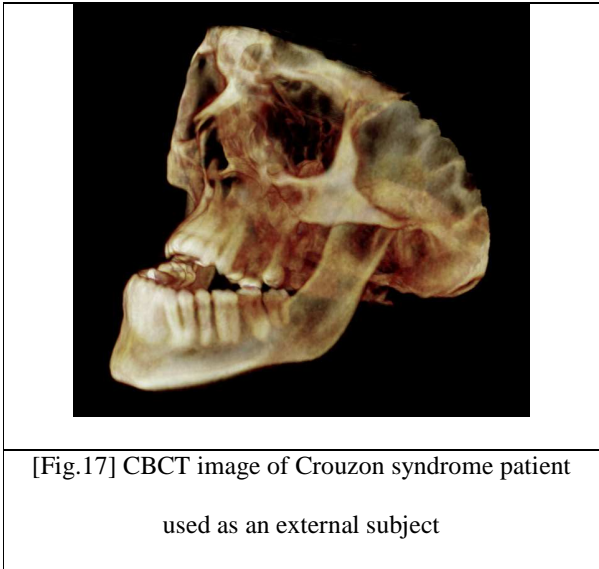
First, Cranial base, Maxillary and Mandibular component were individually superimposed with the normalized component, showing a distinct comparison between the subject and the norm. The visualized image is shown in Fig. 18 and 19 whereas the numberical values for selective points are provided in Table 12 and Table 13 .

[Fig. 18] Non-Size-Standardized Superimposition

of the components of the external subject

(White: external subject, Colored : Norm)

[Fig. 19] Size-Standardized Superimposition of the components of the external subject (White: external subject, Colored : Norm)

Landmark	Subject Coord.			Deviation of Coord.			Dev. of Coord. In STDV			Dev	Dev. in STDV
	x	y	z	x	y	z	x	y	z		
Basion	169.34	117.04	32.92	-0.10	-9.81	1.78	-0.08	-4.67	0.41	9.97	4.47
Nasion	169.41	47.35	57.66	-1.22	-3.96	-0.77	-3.04	-2.86	-0.44	4.22	3.79
Right Fronto-zygomatic	123.46	67.61	56.79	-0.49	2.53	3.94	-0.25	1.36	3.82	4.71	3.12
ANS	171.66	44.33	10.27	1.05	-2.66	4.74	0.95	-0.94	3.82	5.53	3.63
A Point	170.71	51.26	2.43	0.33	4.19	3.58	0.36	3.13	2.32	5.52	5.28
Right Orbitale	138.08	57.86	23.50	1.54	-1.10	-4.72	0.56	-0.91	-2.76	5.08	3.45

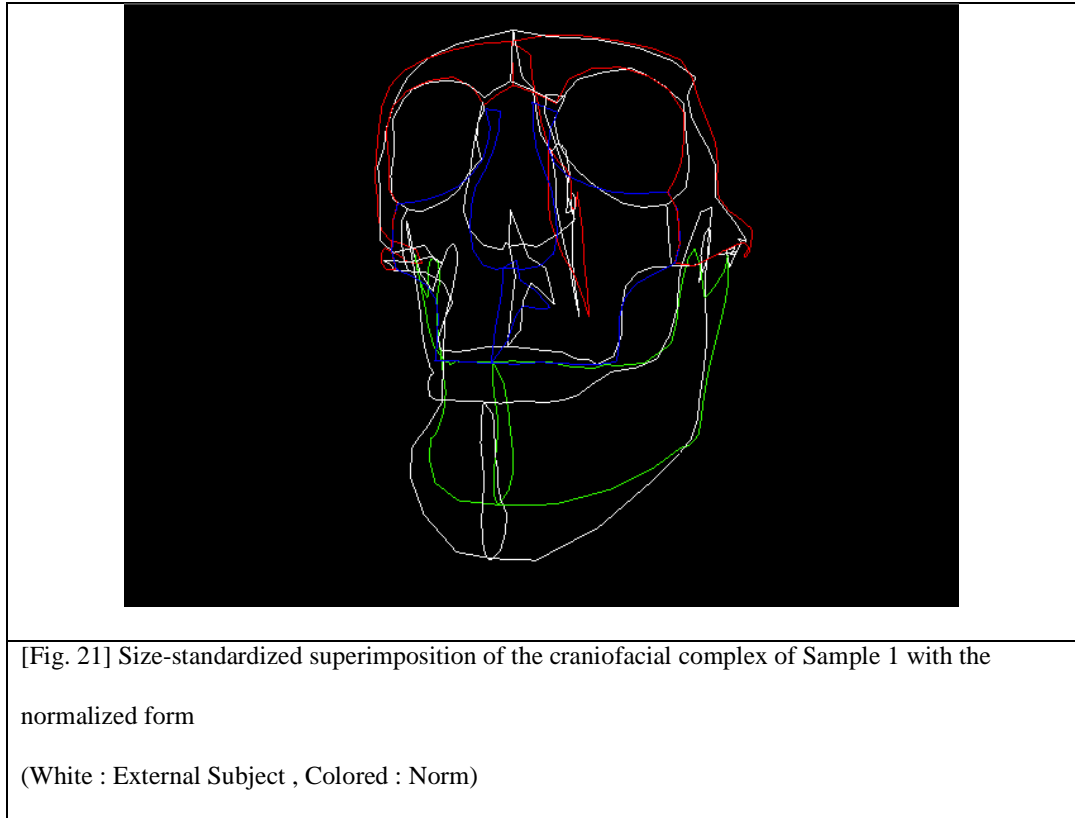| Landmark	Subject Coord.			Deviation of Coord.			Dev. of Coord. In STDV			Dev	Dev. in STDV
	x	y	z	x	y	z	x	y	z		
Rt, Lat. Nasal Cavity	154.05	57.83	17.25	-3.87	4.45	-0.34	-5.92	3.20	-0.15	5.91	3.21
B point	168.63	44.57	-43.59	-0.82	-4.73	-5.24	-2.52	-2.62	-3.40	7.11	5.93
Pogonion	168.56	42.21	-60.13	-0.75	-5.34	-7.43	-1.32	-2.77	-2.97	9.18	4.68
Menton	168.39	48.54	-65.97	-0.82	-3.47	-7.80	-1.30	-1.97	-3.97	8.58	5.37
Rt Gonial Angle	122.91	103.04	-37.07	-0.84	-9.54	-0.24	-0.36	-2.43	-0.12	9.58	3.49
Rt Condylar Head	123.72	126.29	25.17	8.16	4.33	1.69	2.69	4.23	0.72	9.39	4.19

[Table 12] Non-Size-standardized superimposition of the components of the external subject

Landmark	Subject Coord.			Deviation of Coord.			Dev. of Coord. In STDV			Dev	Dev. in STDV
	x	y	z	x	y	z	x	y	z		
Basion	169.33	117.98	32.72	-0.11	-8.87	1.58	-0.09	-3.06	0.37	9.01	3.70
Nasion	169.40	46.38	58.14	-1.23	-4.93	-0.29	-3.21	-2.96	-0.17	5.09	4.37
Right Fronto-zygomatic	122.19	67.20	57.24	-1.76	2.12	4.40	-1.89	1.53	3.77	5.19	6.35
ANS	171.67	44.20	10.25	1.06	-2.78	4.72	0.98	-0.93	3.81	5.58	3.39
A Point	170.71	51.19	2.34	0.33	4.13	3.49	0.36	2.75	2.36	5.41	4.77
Right Orbitale	137.78	57.86	23.60	1.24	-1.10	-4.61	0.58	-0.90	-2.98	4.90	3.53

Rt, Lat. Nasal Cavity	153.89	57.83	17.29	-4.03	4.45	-0.29	-6.31	3.24	-0.13	6.00	3.28
B point	168.58	47.03	-41.94	-0.87	-2.28	-3.59	-2.59	-1.16	-3.29	4.34	3.90
Pogonion	168.52	44.81	-57.46	-0.79	-2.75	-4.76	-1.34	-1.35	-3.27	5.55	4.01
Menton	168.35	50.75	-62.94	-0.85	-1.26	-4.78	-1.32	-0.63	-4.46	5.01	4.63
Rt Gonial Angle	125.67	101.90	-35.82	1.92	-10.68	1.01	0.90	-3.12	0.51	10.90	4.25
Rt Condylar Head	126.43	123.73	22.60	10.86	1.76	-0.88	4.44	0.93	-0.34	11.04	4.92

[Table 13] Size-standardized superimposition of the components of the external subject
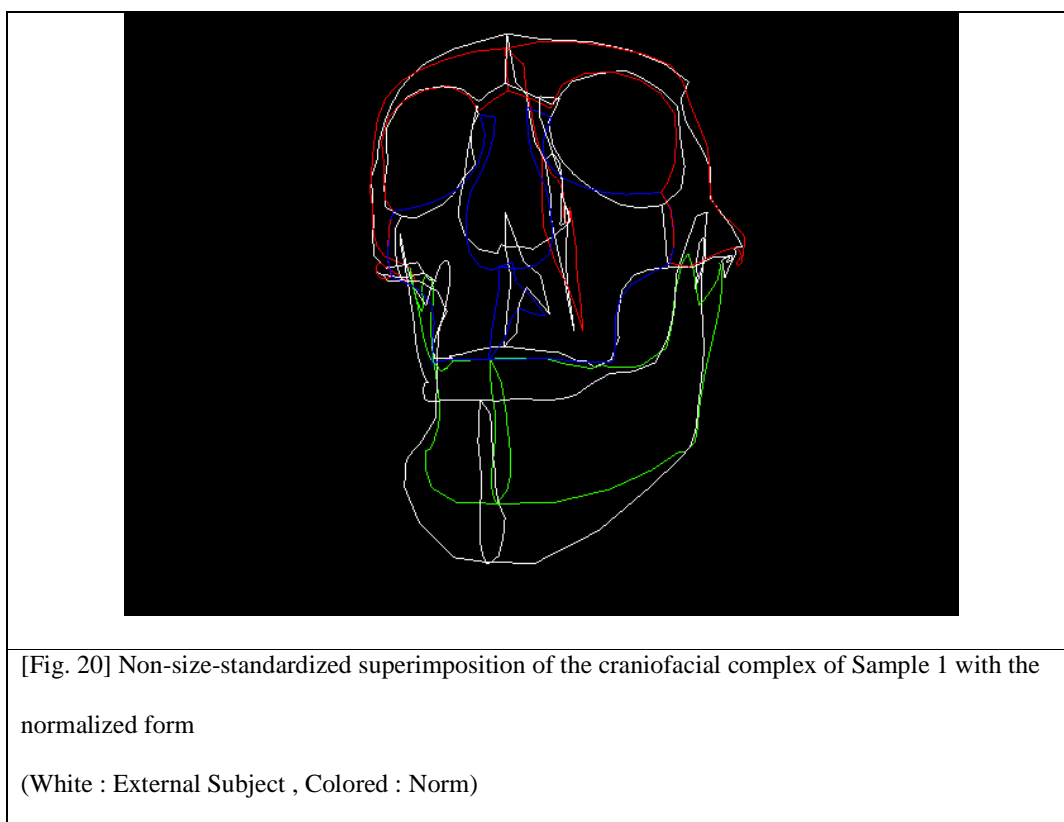
[Fig. 20] Non-size-standardized superimposition of the craniofacial complex of Sample 1 with the normalized form

(White : External Subject , Colored : Norm)

[Fig. 21] Size-standardized superimposition of the craniofacial complex of Sample 1 with the normalized form

(White : External Subject , Colored : Norm)

Landmark	Subject Coord.			Deviation of Coord.			Dev. of Coord. In STDV			Dev	Dev. in STDV
	x	y	z	x	y	z	x	y	z		
Basion	168.92	116.97	32.28	-0.52	-9.88	1.13	-0.43	-4.70	0.26	9.96	4.47
Nasion	170.78	48.07	59.09	0.14	-3.24	0.65	0.35	-2.34	0.37	3.31	2.97
Right Fronto-zygomatic	124.33	67.16	57.75	0.38	2.07	4.90	0.19	1.11	4.76	5.34	3.54
ANS	170.62	51.04	11.98	0.00	4.06	6.46	0.00	1.43	5.20	7.63	5.00
A Point	169.75	58.70	4.85	-0.63	11.64	6.01	-0.68	8.69	3.90	13.11	12.53
Right Orbitale	137.09	63.47	26.37	0.55	4.52	-1.85	0.20	3.73	-1.08	4.91	3.33

Landmark	x	y	z	x	y	z	x	y	z	Dev	Dev. in STDV
Rt, Lat. Nasal Cavity	153.07	63.93	20.19	-4.84	10.55	2.61	-7.40	7.60	1.13	11.90	6.47
B point	168.18	42.77	-51.98	-1.27	-6.53	-13.64	-3.91	-3.62	-8.84	15.17	12.65
Pogonion	168.32	42.74	-68.69	-0.99	-4.82	-15.99	-1.76	-2.50	-6.39	16.73	8.54
Menton	168.44	49.82	-73.59	-0.77	-2.19	-15.43	-1.22	-1.25	-7.86	15.60	9.78
Rt Gonial Angle	124.19	101.25	-37.95	0.44	-11.33	-1.12	0.19	-2.88	-0.57	11.40	4.15
Rt Condylar Head	124.68	115.60	26.93	9.11	-6.37	3.44	3.01	-6.22	1.47	11.64	5.19

[Table 14] None-Size-standardized superimposition of the complex of the external subject

Landmark	Subject Coord.			Deviation of Coord.			Dev. of Coord. In STDV			Dev	Dev. in STDV
	x	y	z	x	y	z	x	y	z		
Basion	168.92	116.56	32.08	-0.51	-10.29	0.94	-0.44	-3.56	0.22	10.35	4.25
Nasion	170.76	48.35	58.62	0.13	-2.96	0.19	0.33	-1.78	0.11	2.96	2.55
Right Fronto-zygomatic	124.79	67.25	57.30	0.84	2.16	4.45	0.90	1.57	3.81	5.02	6.15
ANS	170.61	51.29	11.99	-0.01	4.31	6.47	-0.01	1.44	5.22	7.77	4.73
A Point	169.74	58.88	4.94	-0.64	11.81	6.09	-0.69	7.87	4.12	13.30	11.72
Right Orbitale	137.41	63.60	26.23	0.87	4.64	-1.99	0.41	3.79	-1.28	5.12	3.69

Rt, Lat. Nasal Cavity	153.24	64.06	20.12	-4.68	10.67	2.53	-7.34	7.79	1.12	11.92	6.52
B point	168.19	43.11	-51.33	-1.26	-6.19	-12.98	-3.75	-3.17	-11.90	14.44	12.96
Pogonion	168.33	43.07	-67.87	-0.98	-4.48	-15.16	-1.66	-2.20	-10.42	15.84	11.44
Menton	168.45	50.08	-72.72	-0.76	-1.93	-14.55	-1.17	-0.96	-13.58	14.70	13.57
Rt Gonial Angle	124.65	100.99	-37.44	0.90	-11.59	-0.61	0.42	-3.39	-0.31	11.64	4.54
Rt Condylar Head	125.13	115.20	26.79	9.56	-6.77	3.30	3.91	-3.56	1.28	12.17	5.42

[Table 15] Size-standardized superimposition of the complex of the external subject

4. Discussion

4.1 Significance of the study

Normalization of a group of subjects is an important step for analyzing the irregularity or abnormality of an individual subject by comparison. Traditionally in cephalometrics, the normalized property of a population was given as numerical values derived from multivariate analysis based on edge-superimposition. As discussed above, the most recent attempts have focused on overcoming these constrictions, focusing on the true morphological nature of the anatomical structure [24, 60, 62] . These studies have partially succeded in developing methods to represent part of the craniofacial structures that enabled superimposition or normalization of the craniofacial component. However, the studies were limited to a fraction of the entire facial anatomy, therefore the morphologic information in a broader scope could not be provided. On the other hand, indiscriminately collecting the landmarks from different anatomical regions will not preserve the alignment of each component that is critical for the normalization of the components. Due to the unique characteristics of different anatomic structures in their growth and development, the separation of different anatomical structures is crucial for utilizing the cephalometric image for clinical purposes such as diagnosis and treatment planning

 This study attempted to reconstruct the entire craniofacial complex by combining normalized component of three different segmented anatomical structures. The process of superimposition and normalization of the components inevitably accompanies incoherent affine transformation of the components that result in their separation and misalignment. The irregular arrangement of the normalized components is shown in Fig. 22 . The components were highly coordinated after the inverse transformation method was applied, which provided a reconstructed craniofacial complex (Fig. 23).
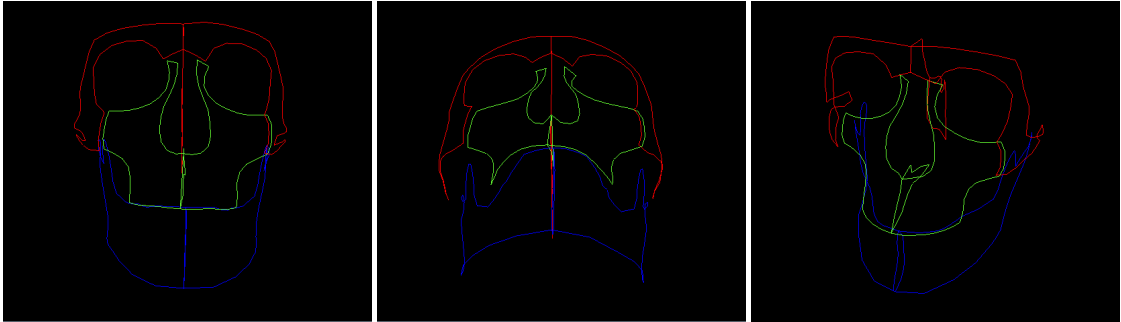
[Fig. 22] Averaged components before realignment
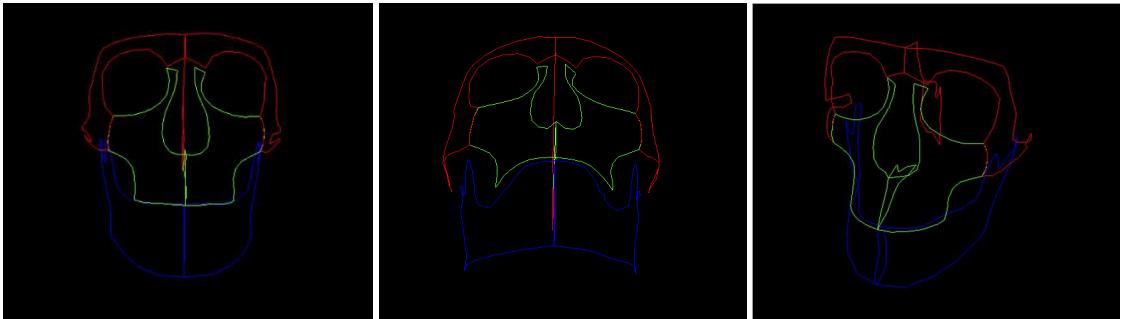
[Fig. 23] Averaged complex reconstructed with the inverse transformation method

A close-up look at the boundaries of the maxilla and zygoma shows that the structures are well aligned with a high degree of accuracy (Fig. 24). Using this method, a representative figure of the entirety of craniofacial structures is established and averaged. Most importantly, each component corresponding to cranial base, maxilla and mandible is a normalized form itself. The averaging process of human craniofacial morphology has never been accomplished, and this model will serve as the first 3-dimensional norm that can be used as a reference for comparing either the individual component or the whole craniofacial complex.

[Fig. 24] A close-up look at the reconstructed normalized craniofacial complex
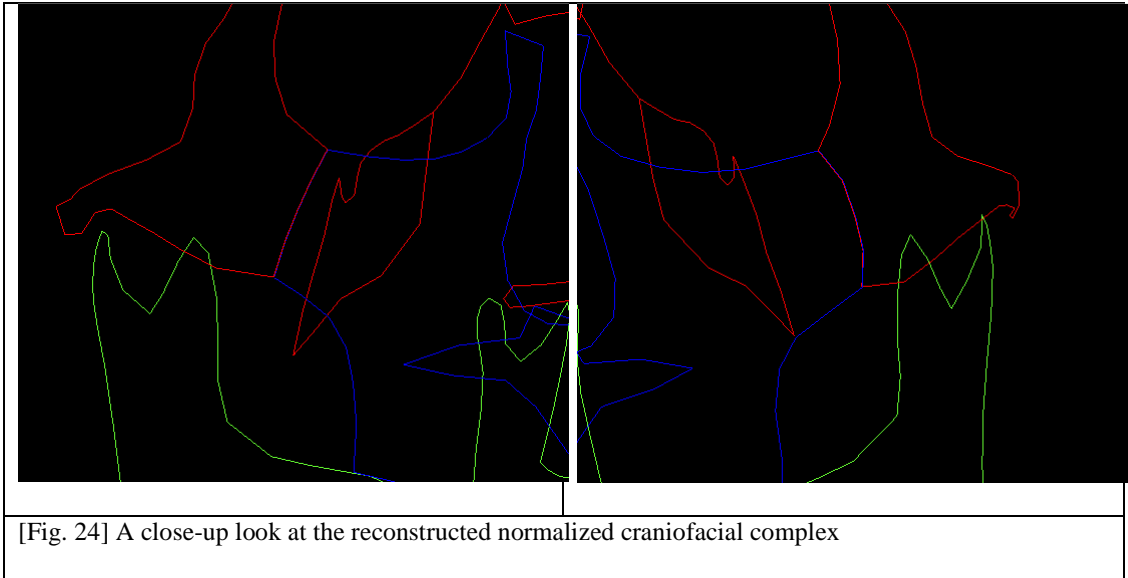
In this study, it was shown that a superimposition of an individual can reveal the difference between the target subject and the norm. Using this method can reveal how far each point along the border of an individual is deviated from the norm. With the statistical data such as the internal variation of the group, the point with an unusual variation can be determined for an individual sample.

The superimposition of each component showed the anatomical variation of the cranial base, maxilla, and mandible, while the superimposition of the whole craniofacial complex showed the morphologic variations when the relative positioning of the components were also taken into consideration. . The comparison was available not only for finding the small variation of an internal subject that was used for generating the norm, but also for an external subject that was greatly deviated from the norm in general.

The superimposition of the subjects was carried out in two different ways: non-size-standardized and size-standardized method. When non-size-standardized superimposition was used, the procedure allowed rigid transformations of the structures without size correction, and is useful when the original structure needs to be preserved. On the other hand, size-standardized superimposition eliminates the size factor, and the variation of shape alone was clearly revealed.

The difference was most obvious in an anatomic structure that had a great size difference, which in this case was the mandible of the external subject (Fig. 25).

[Fig. 25] Non-size-standardized mandible (White) and size-standardized mandible (Blue)
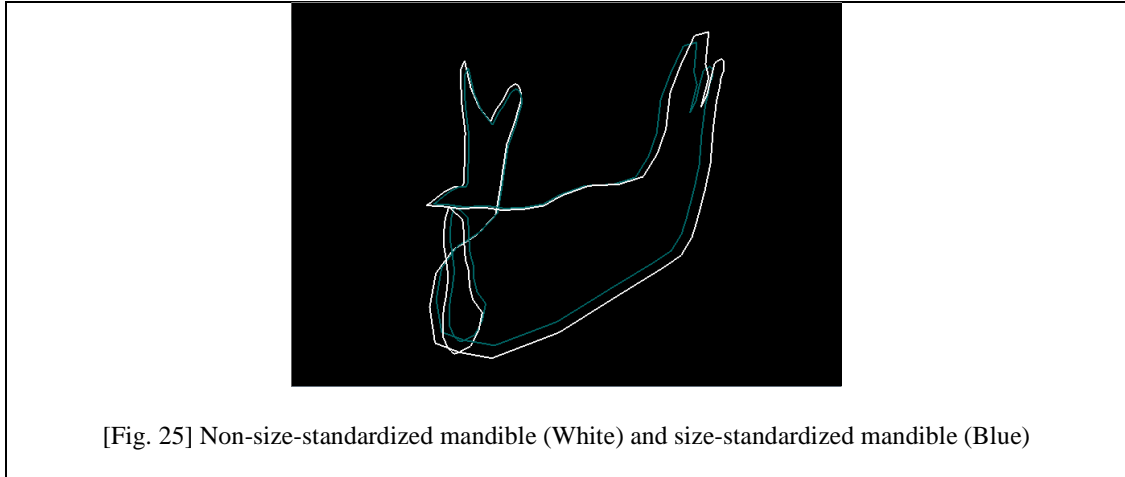
The limitations of conventional cephalometrics have been noted by the clinicians for over decades, and the need of a 3-dimensional analysis has been increasingly gaining attention. As CBCT has been introduced as an effective tool to acquire 3-dimensional skeletal image of the craniofacial area, numerous studies have used different approaches to provide an adequate analytic method to evaluate the subject's morphology. However, a vast majority of the studies have not been successful in capturing the true 3-dimensional figure of the anatomic structures, still relying upon conventional landmarks and their linear measurements. Therefore we have set an essential requirement of a true 3-dimensional analysis as discussed above, and this new approach has shown to be successful in different aspects:

1. The new method has eliminated the excessive dependence on limited landmarks. Instead, the analysis considers each boundary point with equal importance.

2. The geometric figure used in the analysis to describe each anatomic structure represents the actual shape. The craniofacial structure remains as a 3-dimensional entity, and the shape is preserved throughout the process.

3. The analysis provides superimposition of different subjects to provide a normative form and its comparison with individual subjects.

4. The analysis provides statistical results to determine the distinct characteristic of an individual sample.

One of the significant findings of the current analysis is the fact that certain anatomic structures that are assumed to be fixed in conventional cephalometrics are in fact deviated in the current analysis. In the craniofacial complex superimposition, sella was greatly deviated especially in the case of external sample (Fig. 26).

[Fig. 26] Non-size-standardized superimpositions of sample 1 (Left) and the external subject (Right)
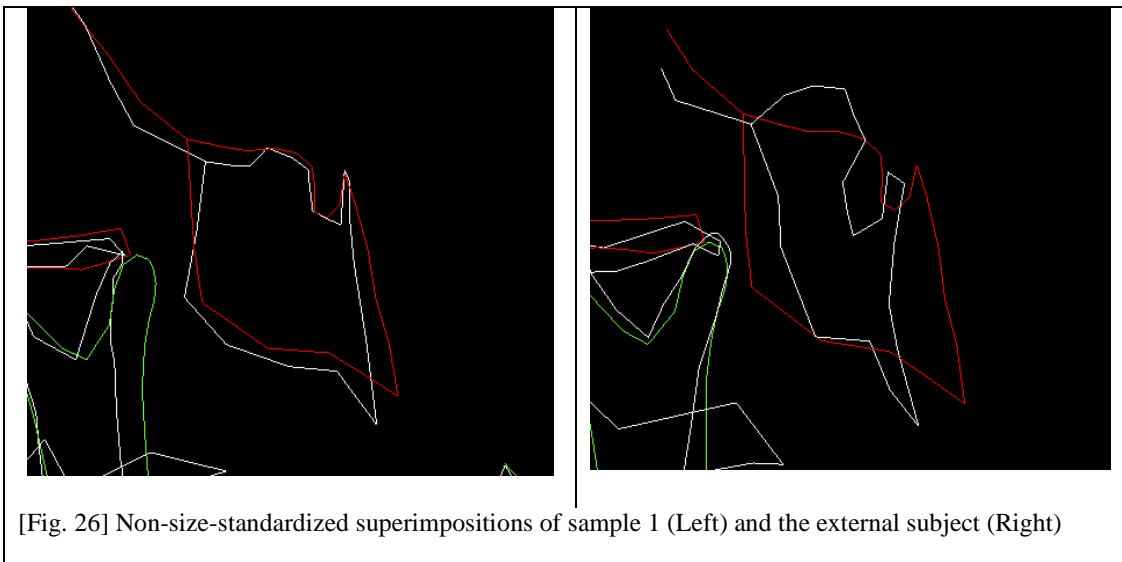
This was expected, since the superimposition is driven by multiple points that define the border of the structure, and lesser points were used to define the sella area which in turn imposes a lesser weighing factor on that specific area. The result is a superimposition that shows a better approximation in the facial area than the sella area. In fact, there is no scientific reason explaining why sella should be the reference for the comparison of craniofacial structures. This analysis

focuses on the area that is of greatest interest; therefore, a true comparison of the morphology is possible.

4.2 Applications and Limitations

The morphologic analysis described in this study has several potential applications.

First, the new method can be used to find normalized morphology of specific population. Human subjects can be categorized by certain factors such as age, gender, ethnicity or even facial patterns, and the general morphologic trait can be extracted from the selected group of subjects. This will provide insight on understanding the true morphologic differences among different populations, and will also be helpful in etting up patient specific treatment goals of orthodontic or surgical correction.

Second, the clinicians treating the patients with orthodontic treatment or orthognathic surgery can use the new analysis to determine which parts of the craniofacial structure are deviated from the norm. In conventional cephalometrics, the result of the analysis is only given by a collection linear measurements and angles, and understanding the nature of the overall morphologic abnormality is extremely unrealisitc. Moreover, the conventional analysis could only represent the 2-dimensional projection of the object, losing the true geometry of the structure. Using the new technique as a tool, the clinicians are now capable of visualizing the defect or abnormality in a 3-dimensional space.

Third, clinical and scientific research is another potential field that this new analysis may be used for. The absence of a regulated protocol for morphological study was the limiting factor for the human skull studies. In previous anthropologic studies, for example, landmark based linear measurements including the conventional cephalometrics were some of the limited number of analytic methods. Using the visual and numerical assistance of the new morphologic analysis, each part of the craniofacial structure can be carefully compared between different subjects or

subgroups, which will allow the researchers to discover unknown variables. This will eventually help scientists and clinicians improve their understandings of the evolution and development of the human face.

The analytic method shown in this study has clear advantages over the conventional cephalometrics, but certain limitations can also be noticed.

In the current analysis, every point in a 3-dimensional structure is used in the registration process for the superimposition. This is useful for finding an overall deviation of the structure, when there is no reliable information of stable points. However, for a subject that has a clear defect only in certain area, the irregularity is evened out over the entire structure and therefore does not show a clear contrast. This will be solved if some of the boundary points can be selectively used for the procrustes superimposition.

Another limitation of the study is that the craniofacial structure cannot be fully described with the boundary information. Surface topology of the craniofacial anatomy is also an important part in evaluating the facial structure. Therefore only when the surface structure is combined with the well-defined border can a complete evaluation be carried out. This analysis is part of the development of a comprehensive morphologic analysis that will follow this study. Ultimately, this boundary mapping study will be combined with the surface mapping study[59] to establish the final 3-dimensional analysis of the human skull. A schematic picture is shown in Fig. 27.
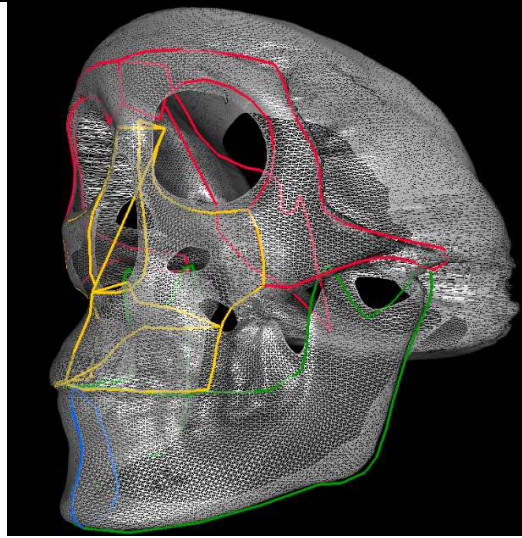
[Fig. 27] An example of Normalized surface and boundary of the craniofacial structure

5. Conclusion

With this novel approach, the average of the craniofacial components and the craniofacial complex can be obtained. The normative structure can be superimposed with individual samples for comparison. This approach provides a basis for a new morphologic analysis that fulfills the requirement of a true 3-dimensional cephalometric analysis and eliminates the limitations of conventional cephalometry. The method described in the study can be improved with the introduction of surface mapping methodology to establish a comprehensive analysis.

6. References

1. Proffit, *Contemporary Orthodontics, 4th Edition*. 2007: Mosby, Inc.
2. Swennen, *Three-dimensional cephalometry : a color atlas and manual*. 2006, Berlin, Newtork: Springer.
3. Moyers, *Handbook of Orthodontics*. 1988, Chicago: Year Book Medical Publishers. 247.
4. Blackith, R., *Multivariate Morphometrics*. 1971, London: Academic Press Inc.
5. Thompson, D.A., *On Growth And Form*. 1942: Cambridge: University Press.
6. K., M., *Contemporary Cephalometric Radiography*. 1996, Tokyo: Quintessence Publishing Co.
7. Athanasiou, *Orthodontic Cephalometry*. 1996: Mosby.
8. Dryden, M., *Statistical Shape Analysis*. 1998, England: John Wiley & Sons Ltd.
9. Bookstein, *Morphometric Tools for Landmark Data - Geometry and Biology*. 1991, New York: Cambridge University Press.
10. Singh J, P.R., *Morphometric sexual dimorphism of human sternum in a north Indian autopsy sample: Sexing efficacy of different statistical techniques and a comparison with other sexing methods.* Forensic Science International, 2013. **228**(1-3): p. 174.e1-174.e10.
11. Cisneiros RA, d.A.A., Melo GR, da Camara CAG, *Morphometric variations in the grasshopper, Chromacris speciosa from two localities of Pernambuco in northeastern Brazil.* J Insect Sci, 2012. **12**.
12. Jungmann PM, T.S., Liebl H, Nevitt MC, McCulloch CE, Lynch J, Link TM, *Association of trochlear dysplasia with degenerative abnormalities in the knee: data from the Osteoarthritis Initiative.* Skeletal Radiol, 2013. **EPub ahead of print**.
13. McNamara, *Cephalometric Superimpositions.* Angle Orthodontist, 2008. **78**(6): p. 967-976.
14. Siegel, *A Robust Comparison of Biological Shapes.* Biometrics, 1982. **38**: p. 341-350.
15. Goodall, *Procrustes Methods in the Statistical Analysis of Shape.* Journal of the Royal Statistical Society. Series B (Methodological), 1991. **53**(2): p. 285-339.
16. Solow, *Cervical and craniocervical posture as predictors of craniofacial growth.* American Journal of Orthodontics and Dentofacial Orthopedics, 1992. **101**: p. 449-58.
17. Duterloo H, P.P., *Handbook of cephalometric superimposition*. 2011: Quintessence Pub Co.
18. Schaefer AT, M.J., Franchi L, Baccetti T, *A cephalometric comparison of treatment with the Twin-block and stainless steel crown Herbst appliances followed by fixed appliance therapy.* Am J Orthod Dentofacial Orthop, 2004.
19. Franco A, M.J., *Class II surgical-orthodontic treatment of a patient with severe coronary disease: 5 years of follow-up.* Am J Orthod Dentofacial Orthop, 2013. **143**(6): p. 855-866.
20. West, *Changes in the craniofacial complex from adolescence to midadulthood: A cephalometric study.* Am J Orthod Dentofacial Orthop, 1999. **115**: p. 521-32.
21. Mihalik CA, P.W., Phillips C, *Long-term follow-up class II adults treatmted with orthodontic camouflage: A comparison with orthognathic surgery outcomes.* Am J Orthod Dentofacial Orthop, 2003. **123**: p. 266-78.
22. Kendall, *Shape and Shape Theory*. 1999, John Wiley & Sons Ltd: England.
23. Chapman, *Conventional Procrustes Approaches*. Proceedings of the Michigan Morphometrics Workshop, Special Publication, ed. Rohlf. 1990: University of Michigan Museum of Zoology.
24. Badawi-Fayad J, C.E., *Three-dimensional Procrustes analysis of modern human craniofacial form.* Anat Rec (Hoboken), 2007. **290**(3): p. 268-76.

25. JF, R., *Statistical power comparisons among alternative morphometric methods.* Am J Phys Anthropol, 2000. **111**: p. 463-478.

26. Smith, *Fluctuating asymmetry in the honey bee, Apis mellifera: effects of ploidy and hybridization.* Journal of Evolutionary Biology, 1997. **10**: p. 551-574.

27. Kearns, *Progression of Facial Asymmetry in Hemifacial Microsomia.* Plast. Reconstr. Surg., 2000. **105**.

28. Suri, *Cranial base, maxillary and mandibular morphology in Down syndrome.* Angle Orthodontist, 2010. **80**(5).

29. You, *Dentoalveolar changes related to mandibular forward growth in untreated class II persons.* Am J Orthod Dentofacial Orthop, 2001. **120**: p. 598-607.

30. Trenouth, *Proportional changes in cephalometric distances during Twin Block appliance therapy.* Eruopean Journal of Orthodontics, 2002. **24**: p. 485-491.

31. Trotman, *Comparison of FAcial Form in Primary Alveolar Bone-Grafted and Nongrafted Unilateral Cleft Lip and Palate Patients: Intercenter Retrospective Study.* Cleft Palate-Craniofacial Journal, 1996. **33**(2).

32. Lambrechts, *Dimensional differences in the craniofacial morphologies of groups with deep and shallow mandibular antegonial notching.* The Angle Orthodontist, 1996. **66**(4): p. 265-272.

33. Jacobson, *The "Wits" appraisal of jaw disharmony.* Am J Orthod Dentofacial Orthop, 1975. **67**: p. 125-38.

34. Kolokitha, *Cephalometric Methods of Prediction in Orthognathic Surgery.* J. Maxillofac. Oral Surg., 2011. **10**(3): p. 236-245.

35. Gu Y, M.J., Sigler L, Baccetti T, *Comparison of Craniofacial Characteristics of Typical Chinese and Caucasian Young Adults.* European Journal of Orthodontics, 2011. **33**: p. 205-2011.

36. Quintero, *Craniofacial imaging in orthodontics: Historical perspective, current status, and future developments.* The Angle Orthodontist, 1999. **69**(6): p. 491-506.

37. Bourriau, *Measurement errors in 2D cephalometrics.* L'Orthodontie Francaise, 2012. **83**(1): p. 23-36.

38. Barbera, *An evaluation of head position and craniofacial reference line variation.* Journal of Comparative Human Biology, 2009. **60**: p. 1-28.

39. Madsen, *Craniofacial reference plane variation and natural head position* European Journal of Orthodontics, 2008. **30**: p. 532-540.

40. Adams, *Comparison between traditional 2-dimensional cephalometry and a 3-dimensional approach on human dry skulls.* Am J Orthod Dentofacial Orthop, 2004. **126**(4): p. 397-409.

41. Halazonetis, *From 2-dimensional cephalograms to 3-dimensional computed tomography scans.* Am J Orthod Dentofacial Orthop, 2005. **127**: p. 627-37.

42. Ludlow, *Precision of cephalometric landmark identification: Cone-beam computed tomography vs conventional cephalometric views.* Am J Orthod Dentofacial Orthop, 2009. **136**: p. 312-3.

43. Hassan, *Precision of identifying cephalometric landmarks with cone beam computed tomography in vivo.* European Journal of Orthodontics, 2013. **35**(38-44).

44. Citardi, *Comparison of Scientific Calipers and Computer-Enabled CT Review for the Measurement of Skull Base and Craniomaxillofacial Dimensions.* Skull Base, 2001. **11**(1): p. 5-11.

45. Haffner, *A technique for three-dimensional cephalometric analysis as an aid in evaluating changes in the craniofacial skeleton.* Angle Orthodontist, 1999. **69**(4): p. 345-8.

46. Cho, *A three-dimensional cephalometric analysis.* J Clin Orthod, 2009. **43**(4): p. 235-52.

47. Park S, Y.H., Kim K, Lee K, Baik H, *A Proposal For A New Analysis Of Craniofacial Morphology By 3-Dimensional Computed Tomography.* Am J Orthod Dentofacial Orthop, 2006. **129**: p. 600.e23-600.e34.

48. Gribel B F, G.M.N., Frazao D C, McNamara J A, Manzi F R, *Accuracy and reliability of craniometric measurements on lateral cephalometry and 3D measurements on CBCT scans.* Angle Orthodontist, 2011. **81**: p. 26-35.

49. Wong R W K, C.A.C.M., Hagg U, *3D CBCT McNamara's cephalometric analysis in an adult southern Chinese population.* Int. J. Oral Maxillofac. Surg., 2011. **40**(9): p. 920-5.

50. de Moraes M E L, H.L.G., Chen C.S.K, Moraes L C, Balducci I, *Evaluating craniofacial asymmetry with digital cephalometric images and cone-beam computed tomogrphy.* Am J Orthod Dentofacial Orthop. **139**: p. e523-e531.

51. Gribel B F, G.M.N., Manzi F R, Brooks S L, McNamara Jr J A, *From 2D to 3D: an algorithm to derive normal values for 3-dimensional computerized assessment.* Angle Orthodontist, 2011. **81**: p. 3-10.

52. Brown A A, S.W.C., Scheetz J P, Silveira A M, Farman A G, *Linear accuracy of cone beam CT derived 3D images.* Angle Orthodontist, 2009. **79**: p. 150-157.

53. Bayome M, P.J.H., Kook Y H, *New three-dimensional cephalometric analyses among adults with a skeletal class I pattern and normal occlusion.* Korean J Orthod, 2013. **43**(2): p. 62-73.

54. Zumpano MP, R.J., *Growth-related shape changes in the fetal craniofacial complex of humans (Homo sapiens) and pigtailed macaques (Macaca nemestrina): a 3D-CT comparative analysis.* Am J Phys Anthropol, 2003. **120**(4): p. 339-51.

55. Nur M, K.S., Bayram M, Celikoglu M, Kilkis D, Sezgin O, *Conventional frontal radiographs compared with frontal radiographs obtained from cone beam computed tomography.* Angle Orthodontist, 2012. **82**(4): p. 579-584.

56. van Vlijmen, K.M., Berge S, Schols J, Maal T, Breuning H, Kuijpers-Jagtman, *Evidence Supporting the Use of Cone-Beam Computed Tomogrphy in Orthodontics.* The Journal of the American Dental Association, 2012. **143**(3): p. 241-252.

57. Dean D, B.F., Koneru S, Lee JH, Kamath J, Cutting CB, Hans M, Goldberg J, *Average African American three-dimensional computed tomography skull images: the potential clinical imporance of ethnicity and sex.* J Craniofac Surg, 1998. **9**(4): p. 348-58.

58. P. N. Gonzalez, V.B., S. I. Perez, *Analysis of Sexual Dimorphism of Craniofacial Traits Using Geometric Morphometric Techniques.* International Journal of Osteoarchaeology, 2011. **21**: p. 82-91.

59. Gutman B, M.R., Sung J,Moon W,Thomson PM, *Robust shape correspondence via spherical patch matching for atlases of partial skull models.* Mesh Processing in Medical Image Analysis, 2012: p. 89-100.

60. W, M., *A numerical and visual approach for measuring the effects of functional appliance therapy: fourier descriptors*. Fourier descriptors and their applications in biology, ed. L. PE. 1997, New York: Cambridge University Press.

61. Lestrel PE, R.D., Wolfe C, *Size and shape of the rabbit orbit: 3-D Fourier descriptors*. Fourier descriptors and their applications in biology, ed. L. PE. 1997, New York: Cambridge University Press.

62. Khullar R, L.P., Moon W, Wolfe CA, *Representation of the mandible as a curve in 3-space: A preliminary study using Fourier descriptors.* Proceedings of the 2nd international symposium of biological shape analysis, ed. L. PE. 2013, Singapore: World scientific.

63. Enlow DH, H.M., *Essentials of facial growth*. 1996, Philadelphia: W.B. Saunders Company.

64. Gower, J.C. and G.B. Dijksterhuis, *Procrustes problems. .* Psychometrika, 2005. **70**(4): p. 799-801.

65. Joshi, S.H., et al., *An efficient representation for computing geodesics between n-dimensional elastic shapes.* IEEE conference on computer vision and pattern recognition, 2007.

66.	Kurtek, S., et al., *Parameterization-invariant shape statistics and probabilistic classification of anatomical surfaces.* Information processing in medical imaging : proceedings of the ... conference, 2011. **22**: p. 147-58.
67.	Karcher, H., *Riemannian center of mass and mollifier smoothing.* Communications on Pure and Applied Mathematics, 1977. **30**(5): p. 509-541.
68.	Woods, R.P., *Characterizing volume and surface deformations in an atlas framework: theory, applications, and implementation.* Neuroimage, 2003. **18**(3): p. 769-788.